São Paulo State University (UNESP)
School of Engineering, Bauru

Gabriella Furlan Nehemy

Dynamic analysis of axially moving cables on elastic supports using the Spectral and Finite Element Methods

July, 2020

Gabriella Furlan Nehemy

Dynamic analysis of axially moving cables on elastic supports using the Spectral and Finite Element Methods

A dissertation presented for the degree of Master of Science at the São Paulo State University (UNESP) in a partial fulfillment of the requirements.

Supervisor: Prof. Dr. Paulo José Paupitz Gonçalves

July, 2020

Nehemy, Gabriella Furlan
N395d Dynamic analysis of axially moving cables on elastic supports using the Spectral and Finite Element Methods / Gabriella Furlan Nehemy. -- Bauru, 2020
88 p. : il., tabs., fotos

Dissertação (mestrado) - Universidade Estadual Paulista (Unesp), Faculdade de Engenharia, Bauru
Orientador: Paulo José Paupitz Gonçalves

1. Axially moving system. 2. Elastic foundation. 3. Periodicity. 4. Spectral Element Method. 5. Finite Element Method. I. Título.

Sistema de geração automática de fichas catalográficas da Unesp. Biblioteca da Faculdade de Engenharia, Bauru. Dados fornecidos pelo autor(a).

Essa ficha não pode ser modificada.

ATA DA DEFESA PÚBLICA DA DISSERTAÇÃO DE MESTRADO DE GABRIELLA FURLAN NEHEMY, DISCENTE DO PROGRAMA DE PÓS-GRADUAÇÃO EM ENGENHARIA MECÂNICA, DA FACULDADE DE ENGENHARIA - CÂMPUS DE BAURU.

Aos 30 dias do mês de julho do ano de 2020, às 09:00 horas, no(a) Via Sistema de videoconferência e outras ferramentas de comunicação a distância, reuniu-se a Comissão Examinadora da Defesa Pública, composta pelos seguintes membros: Prof. Dr. PAULO JOSÉ PAUPITZ GONÇALVES - Orientador(a) do(a) Departamento de Engenharia Mecânica / Faculdade de Engenharia de Bauru - UNESP, Prof. Dr. FABRICIO CESAR LOBATO DE ALMEIDA do(a) Departamento de Engenharia de Biossistemas / Faculdade de Ciências e Engenharia de Tupã - UNESP, Prof. Dr. DOUGLAS DOMINGUES BUENO do(a) Departamento de Matemática / Faculdade de Engenharia de Ilha Solteira - UNESP, sob a presidência do primeiro, a fim de proceder a arguição pública da DISSERTAÇÃO DE MESTRADO de GABRIELLA FURLAN NEHEMY, intitulada **DYNAMIC ANALYSIS OF AXIALLY MOVING CABLES ON ELASTIC SUPPORTS USING THE SPECTRAL AND FINITE ELEMENT METHODS** . Após a exposição, a discente foi arguida oralmente pelos membros da Comissão Examinadora, tendo recebido o conceito final:_ _ _ APROVADA _ _ _ _ . Nada mais havendo, foi lavrada a presente ata, que após lida e aprovada, foi assinada pelos membros da Comissão Examinadora.

Prof. Dr. PAULO JOSÉ PAUPITZ GONÇALVES

Prof. Dr. FABRICIO CESAR LOBATO DE ALMEIDA

Prof. Dr. DOUGLAS DOMINGUES BUENO

I hereby declare that this dissertation has been composed by myself and it has not been submitted for any previous application for a degree. All the work described in this dissertation has been done by myself and all the sources of information have been specifically referenced.

Dynamic analysis of axially moving cables on elastic supports using the Spectral and Finite Element Methods

Gabriella Furlan Nehemy

Keywords: axially moving systems, elastic foundation, periodicity, Spectral Element Method, Finite Element Method

Abstract - In many industrial equipment, axially moving systems are used for transmitting power, transport material or as manufacturing processes. Power transmission belts, textile fibers, band saws, cold drawing process, elevator cables, paper sheets, aerial cable tramways are some examples. In these systems the axial speed plays an important role in changing the dynamic behavior, inducing changes in natural frequencies and vibration modes, thus the main problem that constrains applications in these devices is limiting the transverse vibration caused primarily by the axial moving speed. In this dissertation, different axially moving cables were modeled with simple supports, elastic foundation and periodic elastic foundation using the Spectral Element Method and the Finite Element Method. Dynamic analyses were performed in order to evaluate the influence of the moving speed, the elastic foundation and the periodicity on the dynamics of each model. It was observed that the increasing speed decreases all the resonance and anti-resonance frequencies. The elastic foundation increases the resonance frequency however it has no influence on the anti-resonance frequency of the models. However, for the periodic systems analyzed, when the elastic linear constant of the base is increased, the propagation frequency range become narrower and when there is an increase in axial velocity, the propagation frequency range become smaller.

Análise dinâmica de cabos com movimento axial sobre suportes elásticos utilizando os Métodos dos Elementos Espectrais e Finitos

Gabriella Furlan Nehemy

Palavras chave: sistemas com movimento axial, base elástica, periodicidade, Método dos Elementos Espectrais, Método dos Elementos Finitos

Resumo - Em muitos equipamentos industriais, os sistemas com movimento axial são utilizados para transmitir potência, transportar material ou em processos de fabricação. Correias de transmissão, fibras têxteis, serras fita, processo de trefilação a frio, cabos de elevador, folhas de papel, bondes de cabos aéreos são alguns exemplos. Nesses sistemas, a velocidade axial desempenha um papel importante na alteração do comportamento dinâmico, induzindo alterações nas frequências naturais e nos modos de vibração, portanto, o principal problema que restringe as aplicações nesses dispositivos é limitar a vibração transversal causada principalmente pela velocidade de movimento axial. Nesta dissertação, diferentes modelos de cabo com movimento axial foram desenvolvidos com suportes simples, base elástica e periodicidade da base elástica utilizando os métodos dos elementos espectrais e elementos finitos. Análises dinâmicas foram executadas a fim de avaliar as influências da velocidade do movimento axial, da base elástica e da periodicidade da base elástica no comportamento dinâmico de cada um dos modelos. A partir dos resultados, observou-se que o aumento da velocidade do movimento axial diminui as frequências de resonância e anti-ressonância. A base elástica aumenta a frequência de ressonância porém não tem influência na frequência de anti-ressonância dos modelos. Para o modelo periódico, quando se aumenta a constante linear elástica da base as regiões de propagação ficam mais estreitas e quando há aumento da velocidade axial, as regiões de propagação ficam menores.

Acknowledgements

I would like to thank God for the accomplishment of this dream. I would like to thank everyone who, in some way, contributed to the completion of this dissertation.

First, I would like to thank my supervisor Prof. Dr. Paulo José Paupitz Gonçalves for trusting me, for his guidance, discussions and support during all my research and academic life. My sincerest gratitude! I also would like to thank the committee members Prof. Dr. Fabrício C L de Almeida, Prof. Dr. Douglas D Bueno and Dr. Julio C M Fernandes for your contributions and suggestions to improve this dissertation. I am also grateful to the professors from UNESP that contributed to my formation, in particular Prof. Dr. Marcos Silveira. I am grateful to CAPES (process number: 88882.432805/2019-01) for the financial support. I wish to thank my fellow labmates: Luíza, Carol, Daniel, Gabriel, Sillas, Carlos, Diego, Julio, Willian, Douglas, Matheus, Danilo and Massao for the friendship and support of each one of you. I would like to thank my roommate Luíza R Maniero for all these years of friendship, for the talks, support, kindness and comprehension in our personal and academic life. It was a pleasure to share the home and life with you.

Principalmente, gostaria de agradecer à minha família. Mamãe, Papai, Maga e Caco obrigada por todo amor e por estarem incondicionalmente ao meu lado. Sem vocês não chegaria até aqui e nem poderia sonhar mais alto. Amo vocês! Maga e mamãe, vocês sempre foram exemplo e orgulho para mim. Mulheres fortes e competentes que me inspiram todos os dias a ser a melhor versão de mim mesma e a nunca parar de aprender. Aos meus avós Fada, Zizinho, Dulce, Hugo e Nesmar obrigada pelo amor, pelo apoio e exemplo. Vocês tornaram, e tornam, a jornada mais agradável e prazerosa. Amo vocês!

Contents

List of Tables

List of Figures

Nomenclature

Designation	Explanation
Latin symbols	
A	cross section area
$\mathbf{A^T}$	transpose of **A** matrix
c	axial moving speed
c_{cr}	critical speed
$\mathbf{C_{MT}}$	damping matrix with the transport of mass on the boundary elements
$\mathbf{d}$	displacement vector of the finite element method
f	nodal force on the time domain
F	nodal force amplitude on the frequency domain
$\mathbf{f}$	force vector
f_n	n^{th} natural frequency
$\mathbf{G}$	damping matrix
k	wavenumber
$\mathbf{K}$	stiffness matrix
$\mathbf{K_{MT}}$	stiffness matrix with the transport of mass on the boundary elements
L	cable length
L_p	length between two consecutive periodic supports
$\mathbf{M}$	mass matrix

$\mathbf{N}$	shape function of the finite element method
N_x	axial tension
s	linear elastic constant
$\mathbf{S}$	spectral matrix
$S_{i,j}^{A}$	components of the A element spectral matrix
t	time
T	kinetic energy on the Hamilton's principle
$\mathbf{T}$	transfer matrix
V	strain energy on the Hamilton's principle
w	transversal displacement on the time domain
W	transversal displacement amplitude on the frequency domain
$\mathbf{w}$	displacements vector
W_{MT}	virtual momentum transport of mass across the boundaries on the Hamilton's principle
W_{NC}	virtual work on the Hamilton's principle
x	axial direction

Greek symbols

δ	attenuation constant
ϵ	phase constant
η	Structural damping
λ	eigenvalues of the transfer matrix
μ	propagation constant
ρ	mass density
ω	angular frequency

Abbreviations	
BS	Bragg scattering
CVT	Continuously Variable Transmission
DFT	Discrete Fourier Transform
DOF	Degree of freedom
DSM	Dynamic Stiffness Method
FEM	Finite Element Method
FFT	Fast Fourier Transform
FRF	Frequency reponse function
LR	Local resonance
PID	Proportional integral derivative controller
SAM	Spectral Analysis Method
SEM	Spectral Element Method
STMM	Spectral Transfer Matrix Method

1. Introduction

1.1 Background on axially moving systems

The research on axially moving systems moving at high speeds is motivated due to the wide range of engineering devices that interfaces with axial movement, such as power transmission belts, textile fibers, band saws, cold drawing process, plastic films, elevator cables, paper sheets, aerial cable tramways, etc., some of them are showed on Fig. 1.1.

However, the moving speed can affect the dynamic behavior, inducing changes in natural frequencies and vibration modes, the system can experience strong vibration and dynamic instabilities thus an important limitation that constrains applications in these devices is the amplitude of the transverse vibration. For example, in band saws, the excessive transverse vibration of a blade results in poor cutting accuracy and surface quality, material wastage, gullet cracking, increased downtime and high noise levels. Therefore to understand the axially moving systems is essential because of the problems connected with the dynamic behavior of such systems.

(a) (b) (c)

Figure 1.1: Examples of real devices that interfaces with axially moving structures (a) Band Saw from Timberwolf Tools (Access 07032020) (b) a power transmission belt from Indiamart (Access 07032020) (c) Paper Sheet Cutter Machine from Royal Packing (Access 07032020)

Extensive work concerning axially moving systems can be found in the literature. One of the earliest publications describing the axially moving systems is Sack (1954) wich analyzed the behavior of transverse standing waves for a uniform travelling cable which is pulled over two smooth supports under constant speed and tension. He found that the longitudinal motion of the cable causes a reduction in the resonance frequencies.

Ames et al. (1968) examined the motion of a moving threadline under planar periodic boundary excitation. Numerical solutions of simplified models predicted instabilities of a hard spring nature and experiments showed that the plane motion is truly non-linear and does have a hard spring jump that is basically due to a critical velocity effect. Mote Jr (1968) presented approximate methods for determining the boundaries of the stability-instability regions of long and thin axially moving materials for two cases of parametric excitation. The equations of motion were found by applying the Galerkin method and had their stability investigated by the Hsu method. Naguleswaran and Williams (1968) considered the parametric lateral vibration of band saw and belt driven systems due to the axial tension fluctuation. It was found that the most intense instability of the band occurs when the excitation due to fluctuation in band tension is at twice the lateral natural frequency of the band. The theoretical conclusions were verified experimentally.

Bhat et al. (1982) studied belt with axial movement supported by an elastic base and also

took into account the non-linearities that arise due to the large amplitudes of the transversal vibration and variable tension. Assuming constant speed, it was obtained the solution for the free vibration of the belt between two pulleys and on an elastic base for different constant speed values. The problem was solved using numerical techniques. It was concluded that the response of axially moving belts is not periodic and the system can become unstable when the moving speed approaches the speed of wave propagation in the material.

Yang and Mote Jr (1990) presented a method for active control of band saw vibration. The band saw was modeled as an axially moving cable and the theoretical results were verified experimentally. It was found that vibration in all the modes can be damped through use of only one sensor and one actuator and that the control algorithms presented are carried out in practice. Perkins (1990) investigated the linear dynamics of an axially moving cable when an elastic foundation is added to the problem of axially moving structures. It concluded that the elastic foundation has no effect on the critical speed, but it can significantly change the vibration modes of the structure and therefore, considerably influence the forced response of the cable. Lee and Perkins (1995) conducted experiments with suspended strings moved by harmonic excitation in order to validate theoretical predictions. It was carried out an experiment in which harmonic excitation was applied to the cable, in the equilibrium plane. For some excitation amplitude and frequency excitation ranges, periodic and quasi-periodic responses were observed and qualitatively correspond to theoretical results.

Zhu et al. (1997) developed a spectral analysis for the constrained translating cable with the constrained, represented by mass, stiffness and damping located at an arbitrary position along the span. It was found that when the damping arbitrary position is an irrational number it dissipates vibration energy in all modes and also that with no damping, the cable is stable if and only if the position along the span is an irrational number. Chen (1997) investigated both numerically and analytically the natural frequencies and stability of a cable traveling between two fixed supports and in contact with a static load system, which contains parameters as dry friction, inertia, damping, and stiffness. It was found that the stiffness in the load system tends to increase the natural frequencies of the traveling cable, while the inertia tends to decrease the natural frequencies. Also that the damping element in the load system tends to stabilize

the system in the sub-critical speed range and the large dry friction causes flutter instability in the high speed range, which cannot be suppressed by the damping element in the load system.

Tan and Ying (1997) presented the exact response of an axially moving cable with general boundary conditions based on wave propagation concept. The solution method can include general boundary conditions, it does not require a knowledge of the system eigenfunctions, and it requires much less computation effort compared to the modal analysis method. Furthermore, it also provides a physical interpretation of the response in terms of wave propagation. It was also found that complete wave absorption at a boundary occurs when the boundary has a dashpot with damping coefficient equal to the propagation speed of the reflected wave. Le-Ngoc and McCallion (1999) provide the explicit dynamic stiffness matrix for the transverse oscillation of an axially moving cable under a constant tension using the dynamic stiffness method.

Parker (1999) studied axially moving strings supported on elastic foundation with super-critical speeds, in which the speed is above the critical speed. The elastic foundation introduces additional critical speeds, always greater than the critical speed of strings without a base, and always exhibits divergence above the first critical speed, in contrast to the baseless case in which the balance is stable for all supercritical speeds. Öz and Pakdemirli (1999) investigated the influence of small moving speed oscillations on the stability of an axially moving Euler-Bernoulli beam, assumed harmonic moving speed around a mean value and used the multiple scale method applied to the equation of motion. Pellicano et al. (2001) experimentally investigated the effect of pulley eccentricity on the vibration of a power transmission belt and developed a theoretical model for validation and identification purposes.

Li et al. (2002) used an axially moving cable model to developed a vibration isolation system for web handling machines. The experimental results demonstrate that the exact model knowledge and adaptive controllers outperform PID in impulse response damping and disturbance rejection control efficiency. Pellicano and Vestroni (2002) studied the dynamic response of an axially moving beam subjected to harmonic force within the super critical speed range, namely, at speeds greater than the first critical speed. The discrete model was obtained using the Galerkin method and the results were compared with results found in the literature,

showing agreement on the results. It was investigated in detail the chaotic dynamics and found a cascade of bifurcations, blue-sky catastrophes and also coexisting chaotic and periodic orbits.

Öz (2003) studied the transverse vibration of highly tensioned Euler–Bernoulli beams in contact with a static mass and the effect of mass on different locations were investigated. The linear equations of motion were solved analytically for fixed and simply supported cases. The conclusions obtained were that the mass reduces the frequencies, but the amplitudes of the vibration stay constant and the stationary mass constraint decreases the frequencies through all travelling velocities, but it does not change the critical velocity of the travelling beam. Oh et al. (2004) studied the transversal vibration of an axially moving Euler-Bernoulli beam subjected to axial tensions using the Spectral Element Method. It was also investigated the effects of the moving speed and axial tension on vibration and stability. The accuracy of the Spectral Element Method was verified by comparing numerical with analytical models. It was found that when the moving speed reaches the critical speed the divergence phenomenon occurs, divergence and flutter speeds tend to increase as axial tension is increased and also concluded that there may be a stable region between divergence and flutter zones.

Lee et al. (2004) formulated a spectral element model to analyze the transverse vibration of an axially moving Timoshenko beam subjected to constant axial tension, verified the accuracy of the method by comparing the results with the Finite Element Method and analytical solution and finally investigated the effects of moving speed and axial tension on vibration and stability. Lee and Oh (2005) developed a spectral element model for an axially moving viscoelastic beam subject to axial tension in order to investigate the effects of viscoelasticity and moving speed on system vibration and stability. The SEM (Spectral Element Method) model results were compared with the analytical and the FEM (Finite Element Method) model results. It was concluded that viscoelasticity removes the second stable zone, which appears just after the divergence zone in elastic beams. It was also concluded that the first and second modes gradually change and become similar to each other as the speed is increased. As a result, only the first mode becomes unstable with flutter, unlike elastic beams, where a second coupled flutter mode can occur. Lee and Jang (2007) investigated the effects of the continuously incoming and outgoing semi infinite beam parts on the dynamic characteristics and stability

of an axially moving beam by using the Spectral Element Method and found that the effects of the continuously incoming and outgoing semi-infinite beam parts should be taken into account for accurate prediction of the dynamic characteristics and stability for such axially moving beams.

Banichuk et al. (2014) studied the papermaking process through a simplified model of axially moving materials that provided an understanding of the problem qualitatively and quantitatively. The justification for studying papermaking is that the process is extremely dependent on the efficiency and reliability of the papermaking machine. A multipoint spectral stability problem was formulated with elastic supports and with periodic intervals, the studies were based on analytical approaches. The system stability was investigated using analysis of small periodic transversal displacements. Xia et al. (2015) conducted an experimental study on the nonlinear dynamic characteristics of an axially moving cable. It was concluded that transverse vibrations are highly sensitive to moving speed and initial axial tension applied.

Gaiko and van Horssen (2015) studied the free transverse vibrations of an axially moving material using the model of an axially moving cable with a fixed end and a spring–mass–dashpot system attached to a nonfixed end. It was described explicit approximations of the solution on long timescales by using a multiple-timescales perturbation method and constructed accurate approximations of the lower eigenvalues of the problem, which describe the oscillation and the damping properties of the problem. Zhang and Chen (2016) studied the free and forced response of a cable with axial movement on an elastic base, taking into account foundation damping as well. The study took into account only the linear terms of the governing equations so the solution is only valid for small displacements. Sorokin and Thomsen (2017) analyzed the transverse vibration in an axially moving cable with periodically modulated cross section using the Method of Varying Amplitudes. It was found that due to spatial inhomogeneity, oscillations at a certain distance from the boundary involve many frequencies.

Mao et al. (2017) investigated the internal resonance of the axially moving beam with supercritical speed, subjected to harmonic excitation forces. The equation of motion was derived from the generalized Hamilton principle. Critical excitation of local response was estimated by analytical methods and confirmed by simulations. Banichuk et al. (2018) studied

an infinite beam on identical supports with uniform intervals, as an idealized model that represents the central part of a comprehensive system, that can be represented by several industry systems, such as paper, steel and rubber manufacturing, for example. The supports were modeled linearly, using Hooke's law, and when compared to rigid supports, allows to study the effects of the elasticity foundation on the infinite beam. Axial movement has been suppressed, so the results are only applicable to systems with low speeds, where axial movement can be neglected.

1.2 Background on periodic systems

A system composed of identical units that are repeated is called a periodic structure. the smallest part of a structure that constitutes the repeating pattern are called cells and can be repeated in one, two or three directions. According to Hussein et al. (2014), the spatial periodicity can be in the constituent material phases, or the internal geometry, or the boundary conditions. The mechanical wave propagation in periodic structures has been investigated because of its applications involving vibration and acoustic attenuation and control, energy localization and harvesting. (Brillouin, 1953; Mead, 1996)

The band gap, is the region on the frequency spectrum where waves cannot propagate, this region can be tuned to match expected excitation frequencies and the optimization problems (Hvatov and Sorokin, 2015; Brillouin, 1953). The study of one cell behavior is enough to determine the stop and pass band of the entire structure, independent of the number of cells. According to Zhou et al. (2017), generally, there are two mechanisms to create a band gap, either Bragg scattering (BS) or local resonance (LR). A BS is normally obtained by having two materials within the unit cell or a single material with inserts or discontinuities and through destructive interference it inhibits waves whose wavelength is on the order of the mediums' spatial periodicity (i.e., the Bragg limit), thus the band gap is opened by destructive interference of incident and reflected waves inside the unit cell. The LR does not require the lattice to be periodic, however the wave propagation can be limited using an intrinsic resonance in the unit cell, decoupling the unit cell size from the wavelength of the attenuated waves and thereby enabling subwavelength wave control, the local resonance absorb the energy from the

host structure producing negative dynamic mass or/and stiffness (Foehr et al., 2018; Beli, 2018).

The dispersion relation of a system describes how energy changes, the dispersion curve is the relationship between frequency and the wave vector. When material damping is present, all wave vectors will become complex as energy will be dissipated and the wave will always attenuate. The band gaps can be determined from the dispersion curves, where the band gaps are regions which the imaginary parts do exist and are different from zero. This is because the imaginary parts of the wave vectors represent the attenuation of the waves and a non-zero value for the imaginary part means that the wave is reducing in amplitude after each unit cell (Junyi and Balint, 2015). To find and evaluate the dispersion curves, the transfer matrix can be applied to a single unit cell of the periodic structure and the resulting eigenvalue problem is solved to seek the dispersion curve.

Shen and Cao (2000) used the transfer matrix and Floquet's theorem to derived the dispersion relation for acoustic wave propagation in a periodic layered structure. The calculated results were verified experimentally and good agreement was obtained between the experimental results and the transfer matrix calculations. Lee (2000) introduced a general approach to spectral element formulation for one-dimensional structures, in which the spectral element matrix is computed numerically directly from the transfer matrix formulated from the state vector equation of the structure motion. By combining the promising features of the Spectral Element Method and the well-known transfer matrix, a new solution approach named the spectral transfer matrix method (STMM) was introduced herein. Hussein et al. (2014) made an overview of historical developments and a technical review of recent progress in the field of the dynamics of Phononic materials and structures with special consideration given to aspects pertaining to the fundamentals of dynamics, vibrations, and acoustics. Ashari and Stephen (2019) derived two forms of dynamic transfer matrix (the displacement-force transfer matrix and the displacement-displacement transfer matrix) for a one-dimensional (beam-like) repetitive pin-jointed structure with point masses located at nodal cross-sections. Then, made an exposition the relationships between the two forms of transfer matrix, including their respective advantages and disadvantages.

1.3 Axially moving models studied in this dissertation

The axially moving systems can be found in the industry and some examples of engineering devices were discussed. An important consideration about these systems is the moving speed, which can affect the dynamic behavior, inducing changes in natural frequencies and vibration modes resulting strong vibration and dynamic instabilities. The different types of support that will be analyzed were presented, including simple supports, elastic foundation and periodic elastic foundation, and a literature review was made.

The different configuration used in this dissertation are shown in Fig. 1.2. These configurations are based on the axially moving cable proposed by Lee (2009) with some variation. The cables have constant cross section area (A) and mass density (ρ), are subjected to an axial force (N_x) and have axial moving speed (c).

The first configuration is the Fig. 1.2(a), it has two simple supports and it was studied using both the Spectral Element Method and the Finite Element Method. The system in Fig. 1.2(b) has a simple support in one end and a spring representing a elastic foundation on the other end, and it was analyzed using the Spectral Element Method, the Fig. 1.2(c) is similarly to the first model, except for the elastic foundation on the middle of the cable and it was analyzed using the Spectral Element Method, the Fig. 1.2(d) is the periodic system, it has several periodic elastic foundation between the simple supports and it was analyzed using the Spectral Element Method and then the spectral matrix was transformed into transfer matrix to analyze the dispersion curves.

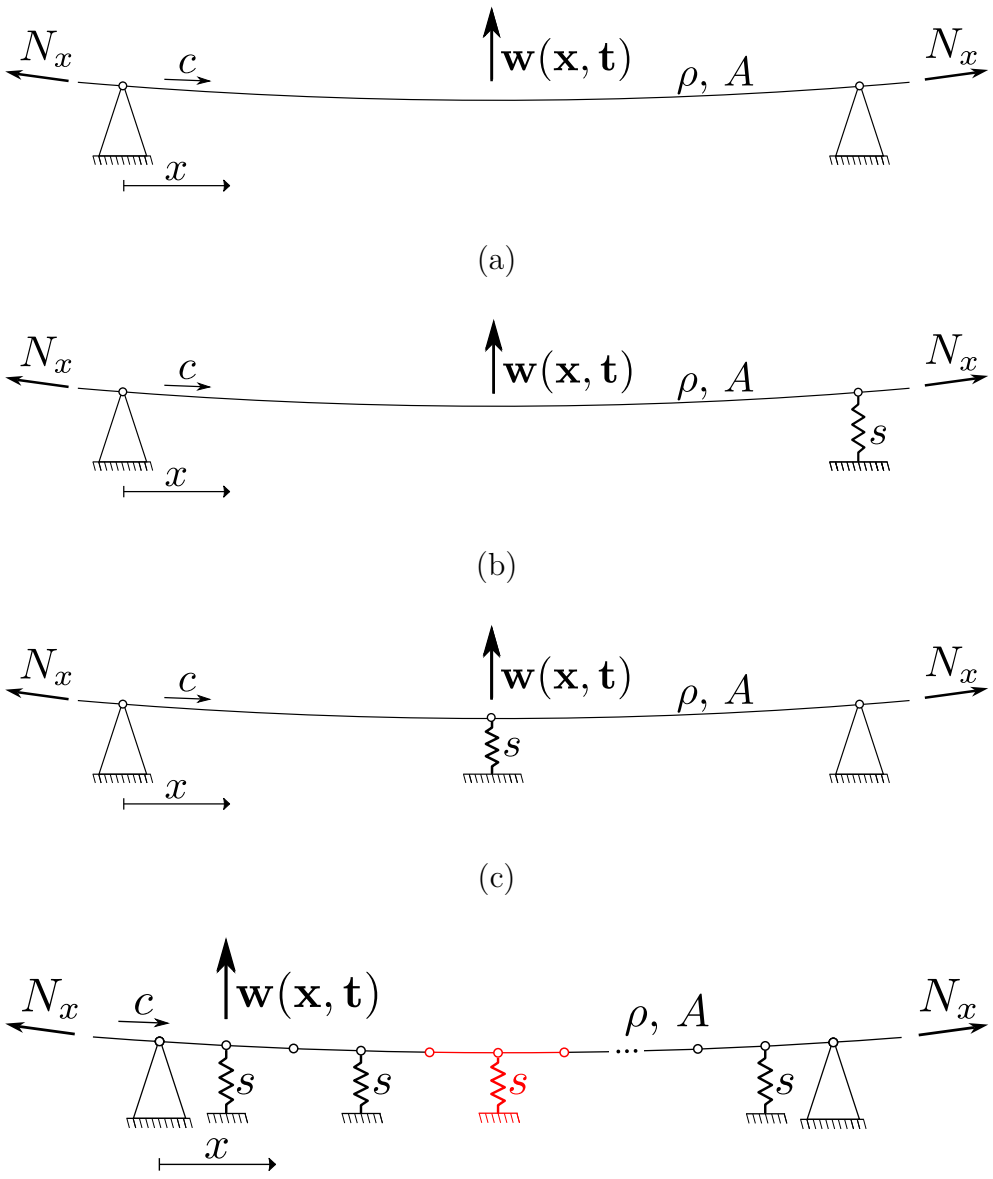

Figure 1.2: The axially moving models studied in this dissertation. (a) simple supported, (b) with one elastic foundation, (c) simple supported with an elastic foundation in the midle of the cable and (d) simple supported with periodic spaced elastic foundations.

1.4 Objectives and Contributions

Starting with the axially moving cable proposed by Lee (2009) and inserting some different configurations, the objectives of this dissertation are:

1. to analyze the influence of the moving speed, the stiffness of the elastic foundation and

the periodicity effects of multiple spring on the dynamics of each model;

2. to compare the results obtained from the different methods used;

Parts of this work have been presented at the 25th International Congress of Mechanical Engineering (COBEM) as Dynamic behavior of axially moving systems with elastic supports (Nehemy et al., 2019).

1.5 Summary of the dissertation

The dissertation is divided in five chapters. This chapter is an introduction to the system studied. Chapter 2 is a review of the methods used. In chapter 3 the mathematical models are implemented using the Spectral Element Method (SEM), based on the model proposed by Lee (2009). Starting with the simple supported model, other features of interest are added, namely the elastic foundation and the periodic elastic foundation. In chapter 4 the numerical analysis performed using the models presented are elucidated and the system behavior are analyzed based on the analysis of frequency response functions (FRFs). For the transfer matrix model, the attenuation and propagation regions are analyzed using the dispersion relation. In chapter 5 conclusions about the results exposed are drawn and some possible approach for further work are shown.

2. Methods for modelling axially moving systems

In the previews chapter, an introduction to the axially moving systems and periodic systems was presented. In this chapter the methods used to describe the axially moving cables were addressed with an introduction and some fundamentals concepts about the method.

Analytical models can fall into two basic categories: continuous models and discrete models. Although continuous systems models are more complex to analysed them lumped parameter systems, they usually provided solutions which are described in terms of analytical functions that can be exact. In some cases, depending on the complexity of the system in analysis, numerical methods must be used. In this context, the Spectral Element Method can be seen as an exact solution of the continuous model system, while other methods, such as, the finite element models can be used, having in mind that they represent approximations of the continuous system model.

2.1 The Spectral Element Method

The Spectral Element Method (SEM) is widely used in solving dynamic structural problems, wave propagation and other related fields as it allows the description of the exact dynamic behavior. The key concept of the Spectral Element Methods was first introduced when Narayanan and Beskos (1978) derived the exact dynamic stiffness matrix of a beam element and employed FFT for the dynamic analysis. Afterward, Spyrakos and Beskos (1982) improved and generalized his work. Doyle (1988) published his first concerning spectral element formulation to rods

longitudinal wave propagation. Nonetheless, the terminology Spectral Element Method was only applied on Rizzi and Doyle (1992). Subsequently, Doyle (1997) published an extensive book on the work they developed. Usik Lee and his students extensively studied the Spectral Element Method applied to several problems developing a wide bibliography regarding it which the majority can be found at (Lee, 2009), but also can be mentioned (Cho and Lee, 2006; Kim et al., 2003; Kwon and Lee, 2006; Lee, 1998, 2000, 2001). A very comprehensive review of the subject can also be found at Wickert and Mote (1988).

According to Lee (2009), the SEM can be seen as a key feature combination of the Finite Element Method (FEM), Dynamic Stiffness Method (DSM) and Spectral Analysis Method (SAM). For the purpose of formulating the dynamic stiffness matrix, the DSM assumes that the dynamic response is a harmonic solution in a single frequency. Whereas the SEM the dynamic responses are assumed to be the superposition of a finite number of wave modes of different discrete frequencies based on the Discrete Fourier Transform (DFT) theory. As well as conventional FEM, the SEM is also an element method, therefore the mesh and mesh refining concepts are also applicable to SEM. The great difference is when the mesh refining is applied, since the SEM gives the exact response, due to its formulation, for a regular structure only one element is needed to represent it, thus, the mesh refining is applied essentially on material and geometrical discontinuities and external forces locations. In contrast to FEM which mesh refining is used to improve the accuracy of the responses, especially on high frequencies. Another feature from FEM is the assembly of the system on a global matrix. The superposition of wave modes via DFT theory and FFT algorithm is a feature from SAM.

2.2 The Finite Element Method

The Finite Element Method is a method for solving engineering problems in several areas. It may be applied in problems such as structural analysis, heat transfer, fluid flow and electromagnetics by computer simulation (Fish and Belytschko, 2000). The method has reached such a state of maturity that it is now thought of as a method for solving general field problems in all areas of engineering and the physical sciences (Gosz, 2017).

The procedure of this method involves three general phases: a pre-processing, an analysis,

and a post-processing. Given the physical problem, the basic idea of this method is to divide the role structure into finite elements, or just elements, connected by nodes and then utilize the relations between the displacements and internal forces at the nodes of the elements to form a global system of equations with the nodal displacements and forces to mathematically represent the real structure. To obtain a sufficiently accurate solution, depending on the the size of the structure thousands of nodes are usually needed , so computers are essential for solving these equations. Generally, the accuracy of the solution improves as the number of elements (and nodes) increases, but the computer time, and hence the cost, also increases (Jacob and Ted, 2007).

The FEM was first introduced in applications to aircraft structural analysis in the mid 1950s, after a series of papers was published by Turner et al. (1956), and during the decade 1945-1955 intensive advances were made in systematic methods for analyzing complex structures which may contain large number of components. Nevertheless, it was Clough (1960) the first to introduce the term "Finite Element Method" (Pian and Tong, 1972; Gosz, 2017). An exceptional work on describing the history of the Finite Element Method has been published by Felippa (2001).

2.3 Chapter remarks

In this chapter the two methods utilized in this dissertation was introduced. The SEM is extensively used in solving dynamic structural problems, wave propagation and other related fields due to its capacity of describing the exact dynamic behavior. The FEM is highly regarded method for solving general field problems in all areas of engineering.

3. System modeling

In this chapter, the mathematical models of the systems introduced in the first chapter were implemented using the Spectral Element Method (SEM), based on Lee (2009), where an axially moving cable was formulated. Starting with the simple supported model from Lee (2009), another features of interest were added, namely the elastic foundation and the periodic elastic foundation.

3.1 Simple supported axially moving cable

The system shown in Fig. 1.2(a) is used as a basis model for comparison with the other problems shown in Fig. 1.2. Mainly, the Spectral Element Method is used to obtain frequency response functions, while other methods, such as the Finite Element Method is used to obtain the equations of motion in state space format, so the stability of the system can be accessed through analysis of the state space matrix eigenvalues.

3.1.1 Spectral Element Method

Figure 3.1 shows a cable with a uniform cross-sectional area A, traveling in its axial direction with a constant speed c with bending (flexural) rigidity considered negligibly small. The simple supports are separated by a distance L, and the cable has mass density ρ, and it is subject to a constant axial tension N_x. The cable undergo a small transverse displacement $w(x,t)$ defined as a function of time and position along the x axis. The simple supports allow the cable to move only on its axial direction x in the supports.

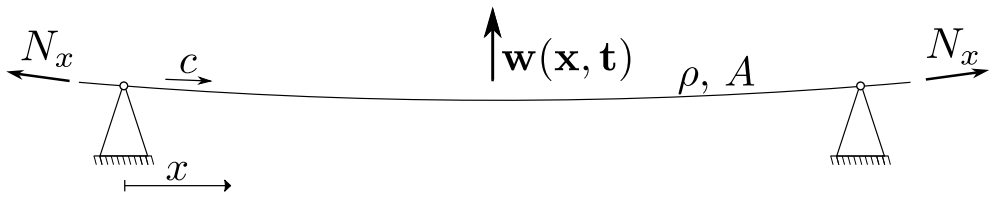

Figure 3.1: Axially moving cables on simple supports. The cable travels in its axial direction x with moving speed c, subjected to an axial tension N_x, with mass density ρ and cross section area A. The simple supports are separated by a distance L and the transverse vibration is given by $\mathbf{w(x,t)}$.

Lee (2009) used the extended form of Hamilton's principle, Eq. 3.1, to derive the governing equation of motion and associated boundary conditions. Where T is the kinetic energy, V is the strain energy, δW_{NC} is the virtual work done by non-conservative external forces, and δW_{MT} is the virtual momentum transport of mass across the boundaries at $x = 0$ and L.

$$\int_{t_1}^{t_2} (\delta T - \delta V + \delta W_{NC} - \delta W_{MT})\, dt = 0 \tag{3.1}$$

After substituting the expressions on the Eq. 3.1 and, after mathematical manipulations, which can be found in Lee (2009), the equation of motion for the axially moving cable, without considering any of the boundary conditions is given by the partial differential equation

$$\rho A\ddot{w} + 2\rho Ac\dot{w}' + \rho Ac^2 w'' - N_x w'' = f(x,t) \tag{3.2}$$

The w' are the spatial derivative and the $\dot{w}$ the time derivative. The solution of Eq. 3.2 is obtained by the method of separation of variables, considering harmonic motion in the time domain as,

$$w(x,t) = W(x)e^{i\omega t} \tag{3.3}$$

The term $W(x)$ is the amplitude and i is the imaginary unit defined by its property $i^2 = -1$. This way, the resulting equation of motion in the frequency domain is obtained as

$$-\omega^2 \rho AW + i2\omega\rho AcW' - (N_x - \rho Ac^2)W'' = F(x) \tag{3.4}$$

Initially, considering the case of free motion ($F(x) = 0$), a solution for the ordinary differential equation (Eq. 3.4) can be written as $W(x) = a\,\mathrm{e}^{-ikx}$, where a is a constant and k is the wavenumber given in rad/m. Applying this expression in Eq. 3.4, it is possible to obtain the dispersion equation

$$\left(N_x - \rho A c^2\right) k^2 + 2\rho A c \omega k - \rho A \omega^2 = 0 \tag{3.5}$$

The wavenumber is calculated solving Eq. 3.5 as

$$k_{1,2} = -\omega \left(\frac{\rho A c \pm \sqrt{N_x \rho A}}{N_x - \rho A c^2} \right) \tag{3.6}$$

$$k = \frac{\omega}{a} \tag{3.7}$$

The difference between the two wavenumbers, k_1 and k_2, is the signal on the numerator, it correspond to number of waves that propagate in the forward direction and other correspond to waves that propagate in the backward direction. Considering the wavenumber denominator, Eq. 3.6, and the parameters that compose it, part of them are cable's physical characteristics, ρ and A, and therefore do not change, the axial tension acting on the cable, N_x, is a system's parameter used so that the cable remains stretched, and therefore, considered constant as well. While the moving speed, c, is not fixed, there is a value that vanishes the expression of the denominator, called the critical speed, Eq. 3.8. When the system achieves the critical speed it becomes unstable and can experience strong vibration. Considering constant axial tension is an ideal situation. On the practice, there is always at least some oscillation, however we are assuming it constant during all the modeling on this dissertation.

$$c_{cr} = \sqrt{\frac{N_x}{\rho A}} \tag{3.8}$$

Applying the boundary conditions for the simple supported model, the natural frequency equation is given in Lee (2009) as

$$f_n = \frac{\omega_n}{2\pi} = \frac{n\left(N_x - \rho A c^2\right)}{2L\sqrt{\rho A N_x}} \tag{3.9}$$

The natural frequency in $[radians/second]$ is found from Eq. 3.9,

$$\omega_n = f_n 2\pi = \frac{N_x - \rho A c^2}{L\sqrt{\rho A N_x}}\pi n \tag{3.10}$$

The normal modes equation is obtained using the wavenumbers equation, Eq. 3.6, on the natural frequency ω_n, as

$$\phi = \sin(k_1 x) - \sin(k_2 x) \tag{3.11}$$

Using the axially moving cable with simple supports, a simulation was performed in order to illustrate the concept of the critical speed, and the main concern about the axially moving systems which is the instability that these systems can experience. Figure 3.2 shows the first four natural frequencies behaviors according to the normalized speed, when the moving speed is equal to the critical speed, all the natural frequencies approach zero, characterizing instability.

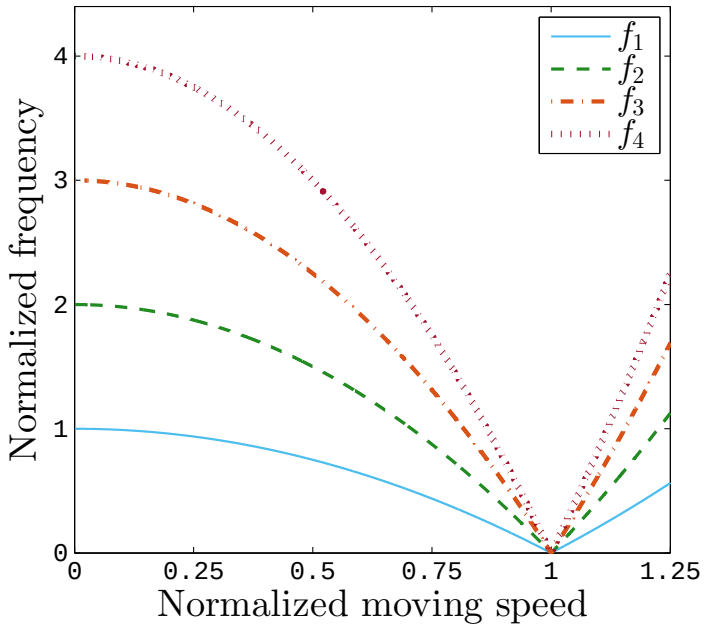

Figure 3.2: The influence of the moving speed on the axially moving cable with simple supports: the behavior of the normalized frequency as the normalized moving speed (c/c_{cr}) increases.

When the cable reaches the critical speed a static instability occurs and the cable seems to remain static. The effects of the moving speed changes can also be seen on the mode shapes. Figure 3.3 shows the first mode shape of the axially moving cable with simple supports. The

blue line represent the stationary system, with no axial movement, and the other lines show systems with partial speed in relation to the critical speed (25%, 50%, 75% and 99%). As the speed increases, the natural frequency of the system decreases and so the modes of vibration change.

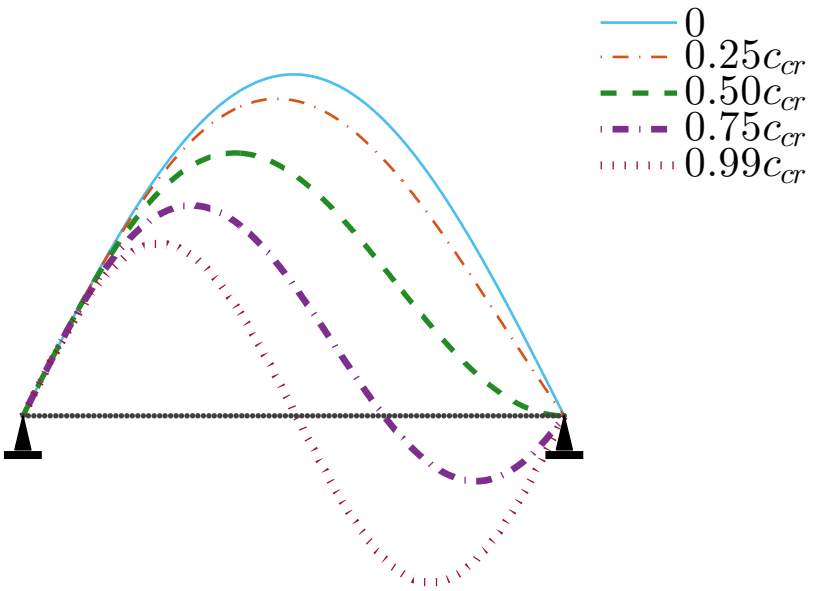

Figure 3.3: The influence of the moving speed on the axially moving cable with simple supports: the first mode shape of the cable for different moving speed of the system.

When

3.2 Harmonic excitation

Considering the case of harmonic force excitation, the cable spectral element matrix can be calculate according the procedure described in Lee (2009), where for one element, the force vector $\mathbf{f}$ is related to the displacements $\mathbf{w}$ at the two ends of the cable, by the spectral element matrix $\mathbf{S}$ as

$$\mathbf{f}(\omega) = \mathbf{S}(\omega)\mathbf{w}(\omega), \quad \text{where, } \mathbf{S}(\omega) = \mathbf{H}(\omega)^{-T}\mathbf{D}(\omega)\mathbf{H}(\omega)^{-1} \tag{3.12}$$

The spectral element matrix is calculated using

$$\mathbf{H} = \begin{bmatrix} 1 & 1 \\ \mathrm{e}^{-ik_1 L_e} & \mathrm{e}^{-ik_2 L_e} \end{bmatrix} \tag{3.13}$$

and,

$$\mathbf{D}(\omega) = -(N_x - \rho A c^2)\mathbf{KEK} - \rho A \omega^2 \mathbf{E} - \omega \rho A c(\mathbf{KE} - \mathbf{EK}) + i\rho A c(\omega \mathbf{I} - c\mathbf{K})\bar{\mathbf{E}} \tag{3.14}$$

L_e is the element length, the matrix $\mathbf{K}$ is a diagonal matrix defined as $\mathbf{K} = \mathrm{diag}(k_1, k_2)$, the elements of the matrix $\mathbf{E}$ are computed as

$$E_{rs} = \begin{cases} \frac{i}{k_r + k_s}\bar{E}_{rs}, & \text{if } k_r + k_s \neq 0 \\ L_e, & \text{if } k_r + k_s = 0 \end{cases} \tag{3.15}$$

where $\bar{E}_{rs}$ are the elements of the matrix $\bar{\mathbf{E}}$

$$\bar{\mathbf{E}} = \begin{bmatrix} \mathrm{e}^{-i2k_1 L_e} - 1 & \mathrm{e}^{-i(k_1+k_2)L_e} - 1 \\ \mathrm{e}^{-i(k_1+k_2)L_e} - 1 & \mathrm{e}^{-i2k_2 L_e} - 1 \end{bmatrix} \tag{3.16}$$

The spectral element matrices can be assembled in a completely analogous way to that used in FEM in order to obtain the global system matrix. Applying the boundary conditions after the assembly may provide a global system equation in the form as

$$\mathbf{S}_g(\omega)\mathbf{w}_g = \mathbf{f}_g \tag{3.17}$$

where $\mathbf{S}_g(\omega)$ is the global dynamic stiffness matrix, $\mathbf{w}_g$ is the global spectral nodal DOFs vector, and $\mathbf{f_g}$ is the global spectral nodal forces vector.

To solve the simple supported system, the boundary conditions must be applied and, since the two end are fixed, for mathematical reasons, this model needs to be developed using two elements as Fig. 3.4, although it is not necessary in terms of discretization.

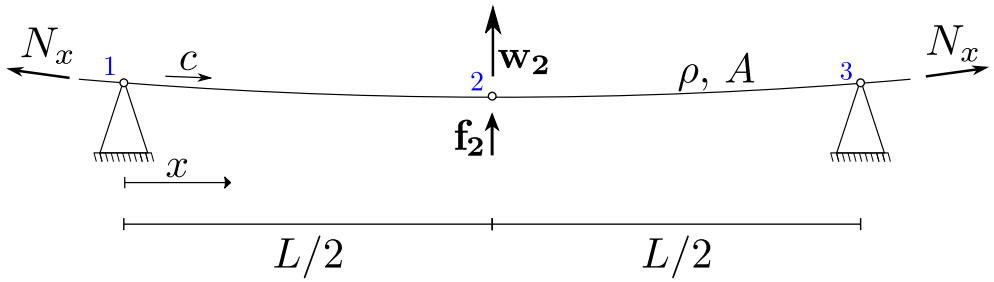

Figure 3.4: The axially moving cable with two elements used to develop the mathematical model. The cable is subjected to an axial force N_x, a constant moving speed c and a harmonic excitation force $\mathbf{f_2}$. The $\mathbf{w_2}$ represents the displacement of the second node.

The cable has an axial tension N_x, travels with a constant moving speed c, has the mass density ρ and the cross-sectional area A. The nodes 1 and 3 are defined at the top of the simple supports and node 3 is in the middle of the cable, each element has length $L_e = L/2$. Thus, the system matrix can be written as

$$\begin{Bmatrix} F_1 \\ F_2 \\ F_3 \end{Bmatrix} = \begin{bmatrix} S^A_{1,1} & S^A_{1,2} & 0 \\ S^A_{2,1} & S^A_{2,2} + S^B_{1,1} & S^B_{1,2} \\ 0 & S^B_{2,1} & S^B_{2,2} \end{bmatrix} \begin{Bmatrix} W_1 \\ W_2 \\ W_3 \end{Bmatrix} \tag{3.18}$$

where $S^A_{i,j}$ are the components of the first element spectral element matrix and $S^B_{i,j}$ are the components of the second element spectral element matrix, given by Eq. (3.12). The application of the simple supported case, allows to write the displacement of the right hand side due to a harmonic force applied at the same location as

$$W_2 = (S^A_{2,2} + S^B_{1,1})^{-1} F_2$$

where, $S^A_{2,2} + S^B_{1,1}$, represents the spectral element equation for the second node of Fig. 3.4.

3.2.1 Finite Element Method

The Finite Element Method can be summarized into five steps. The first is the preprocessing that consists in subdividing the model in finite elements, on this dissertation the amount of elements needed for satisfactorily discretizing the problem was found empirically and will be

shown in subsequent sessions. The second step is the element formulation, the development of equations that describe the elements, in this dissertation it was used the Galerking method, since the physical formulation of the problem is given by a differential equation. The third step is to obtain the global matrix from the element matrices. The fourth step is solving the equations and finally the fifth is the postprocessing, to analyse the results obtained. Considering the shape function $N(x)$ and the nodal displacements $d(t)$,

$$N(x) = \begin{bmatrix} 1 - \frac{x}{L} & \frac{x}{L} \end{bmatrix} \tag{3.19}$$

$$w(x,t) = \mathbf{N}(x)\mathbf{d}(t) \tag{3.20}$$

From the equation of motion in the time domain, Eq. 3.2, the weak form is given by Lee (2009)

$$\int_0^L \left[\left(N_x - \rho A c^2 \right) w' \delta w' + \rho A c \ddot{w} \delta w + \rho A c \left(\dot{w}' \delta w - \dot{w} \delta w \right) \right] dx + \rho A c \left(\dot{w} + c w' \right) \delta w \mid_0^L - Q(x,t) \delta w \mid_0^L - \int_0^L f(x,t) \delta w dx = 0 \tag{3.21}$$

Substituting Eq. 3.20 and 3.19 into Eq. 3.21 the finite element equation was obtained,

$$\mathbf{M}\ddot{\mathbf{d}}(t) + (\mathbf{G} + \mathbf{C_{MT}})\dot{\mathbf{d}}(t) + (\mathbf{K} + \mathbf{K_{MT}})\mathbf{d} = \mathbf{f_c}(t) + \mathbf{f_d}(t) \tag{3.22}$$

where

$$\mathbf{f_d}(t) = \int_0^L f(x,t)\mathbf{N}^T(x)dx \tag{3.23}$$

$$\mathbf{M} = \frac{\rho A L}{6} \begin{bmatrix} 2 & 1 \\ 1 & 2 \end{bmatrix} \tag{3.24}$$

$$\mathbf{K} = \frac{N_x - \rho A c^2}{L} \begin{bmatrix} 1 & -1 \\ -1 & 1 \end{bmatrix} \tag{3.25}$$

$$\mathbf{K_{MT}} = \frac{\rho A c^2}{L} \begin{bmatrix} 1 & -1 \\ -1 & 1 \end{bmatrix} \tag{3.26}$$

$$\mathbf{G} = \rho A c \begin{bmatrix} 0 & -1 \\ 1 & 0 \end{bmatrix} \tag{3.27}$$

$$\mathbf{C_{MT}} = \rho A c \begin{bmatrix} -1 & 0 \\ 0 & 1 \end{bmatrix} \tag{3.28}$$

The finite element matrices were calculated using the equation given on Lee (2009), however the **G** obtained has different signal. For the numerical simulations it was used the calculated damping matrix, Eq. 3.27. On (Lee, 2009) it is given as

$$\mathbf{G} = \rho A c \begin{bmatrix} 0 & 1 \\ -1 & 0 \end{bmatrix} \tag{3.29}$$

Using the FEM mass and stiffness matrices it is possible to obtain the dynamic stiffness matrix, which it is going to be used on the numerical analysis.

$$\mathbf{S} = -\omega^2 \mathbf{M} + (\mathbf{K} + \mathbf{K_{MT}}) \tag{3.30}$$

3.3 Axially moving cable with elastic foundation

In this section, the axially moving models with elastic foundation, Fig. 1.2(b) and Fig. 1.2(c), were developed. The difference between these models and the model showed on the previews section is that the elastic foundation allows the cable to move on both directions, the axial and the transversal, however it offers resistance to transversal movement due to the stiffness of the spring. The both models were developed using the SEM.

3.3.1 Spectral Element Method

The inclusion of a mass, spring or damper component on a node of an impedance matrix is showed on Appendix A. Since the Spectral Matrix is an impedance matrix, to insert the elastic foundation on the model is done by adding the linear stiffness constant s to the node.

Boundary elastic foundation

Considering the case of a cable simple supported at the left hand side and elastically supported on the right hand side by a spring with linear elastic constant s as showed on Fig. 3.5.

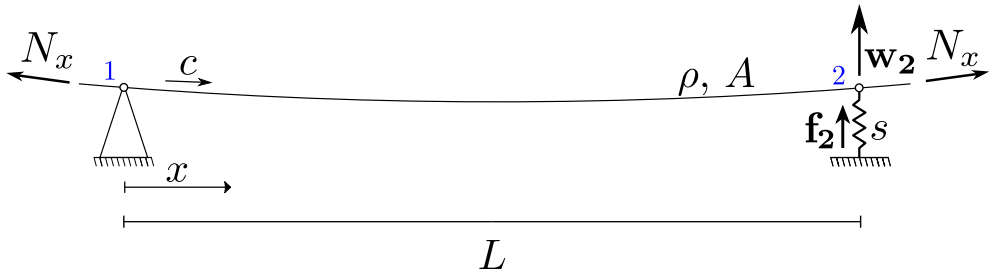

Figure 3.5: The axially moving cable with elastic foundation used to develop the mathematical model. The cable is subjected to an axial force N_x, a constant moving speed c and a harmonic excitation force $\mathbf{f_2}$. The $\mathbf{w_2}$ represents the displacement of the second node.

This model is given by the simple supported model with the add of the elastic foundation impedance. Considering one element to develop this model, the spectral global matrix is given by

$$\left\{ \begin{array}{c} F_1 \\ F_2 \end{array} \right\} = \left[\begin{array}{cc} S_{1,1} & S_{1,2} \\ S_{2,1} & S_{2,2}+s \end{array} \right] \left\{ \begin{array}{c} W_1 \\ W_2 \end{array} \right\} \tag{3.31}$$

The application of the simple supported case, allows to write the displacement of the right hand side due to a harmonic force applied at the same location as

$$W_2 = S_{2,2} + s^{-1} F_2 \tag{3.32}$$

Middle span elastic foundation

Considering the case of a cable simple supported at ends and elastically supported on the middle as showed on Fig. 3.6. Four elements having the same length (L/4) are used to investigate this case, in order to have the cable response at positions in between the node where the spring is attached and the boundaries. The total length of the cable is $L = 2m$.

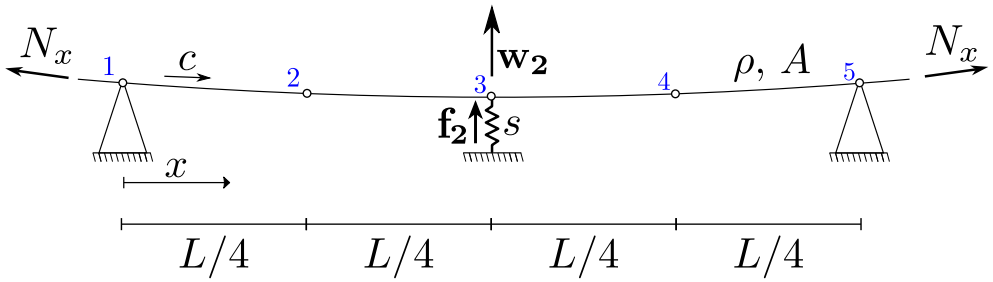

Figure 3.6: The axially moving cable with elastic foundation used to develop the mathematical model. The cable is subjected to an axial force N_x, a constant moving speed c and a harmonic excitation force $\mathbf{f_2}$. The $\mathbf{w_2}$ represents the displacement of the third node.

The development of this model begins with the implementation of the axially moving cable with four elements, as showed on Fig. 3.7.

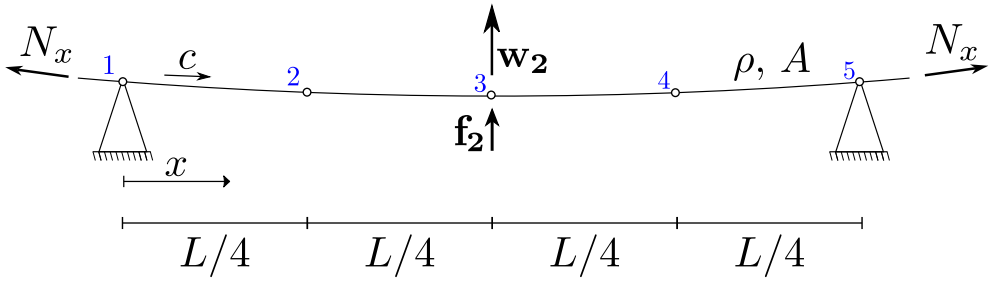

Figure 3.7: The axially moving cable with four elements. The cable is subjected to an axial force N_x, a constant moving speed c and a harmonic excitation force $\mathbf{f_2}$. The $\mathbf{w_2}$ represents the displacement of the third node.

Since the model has four elements it has five nodes, and the system's global spectral matrix is of order five with a diagonal sum of the spectral element matrices as

$$\begin{bmatrix} S^1_{1,1} & S^1_{1,2} & 0 & 0 & 0 \\ S^1_{2,1} & S^2_{2,2}+S^2_{1,1} & S^2_{1,2} & 0 & 0 \\ 0 & S^2_{2,1} & S^2_{2,2}+S^3_{1,1} & S^3_{2,1} & 0 \\ 0 & 0 & S^3_{2,1} & S^3_{2,2}+S^4_{1,1} & S^4_{1,2} \\ 0 & 0 & 0 & S^4_{2,1} & S^4_{2,2} \end{bmatrix} \tag{3.33}$$

with $S^n_{i,j}$ being the spectral matrix components of the n element. The elastic foundation is added on the third node by the sum of the impedance stiffness on the global spectral matrix.

Since the two ends of the model are fixed, the displacement is calculated by

$$\begin{bmatrix} X_2 \\ X_3 \\ X_4 \end{bmatrix} = \begin{bmatrix} S^2_{2,2} + S^2_{1,1} & S^2_{1,2} & 0 \\ S^2_{2,1} & S^2_{2,2} + S^3_{1,1} + s & S^3_{2,1} \\ 0 & S^3_{2,1} & S^3_{2,2} + S^4_{1,1} \end{bmatrix}^{-1} \begin{bmatrix} F_2 \\ F_3 \\ F_4 \end{bmatrix} \tag{3.34}$$

with X_n the amplitude displacement and F_n the amplitude force applied on the original n node on the frequency domain.

3.4 Preliminary axially moving cable with periodic elastic foundation

A preliminar axially moving cable with periodic elastic foundation was also studied using the Spectral Element Method. This model, Fig. 3.8, has some differences from the model presented on Section 4.5. This model was used as a first attempt to understand the dynamic behavior of the periodic elastic foundation supports. However, in order to analyze the periodic model using also the transfer matrix it was necessary to well define the periodic cell, so this model was adapted and transformed into the model on Fig. 1.2(d).

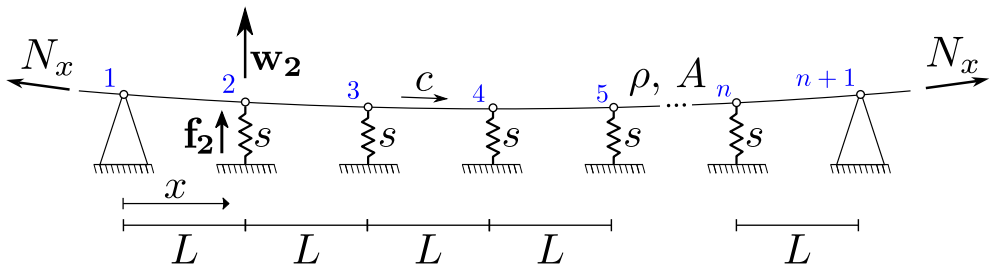

Figure 3.8: The preliminar axially moving cable with periodic elastic foundation model. The cable is subjected to an axial force N_x, a constant moving speed c and a harmonic excitation force $\mathbf{f}$. The $\mathbf{w_2}$ represents the displacement of the second node.

In this model the cell concept is not very well defined, but the elastic foundations are separated by a distance $L = 2\,m$. The model was constructed with 21 nodes, the distance between each node is $L = 2\,m$, so each node has an elastic foundation, except the first and the last, and the entire model has $40\,m$.

The spectral matrix is given by

$$\begin{bmatrix} S_{1,1} & S_{1,2} & \cdots & S_{1,n-1} & S_{1,n} \\ S_{2,1} & S_{2,2}+s & \cdots & S_{2,n-1} & S_{2,n} \\ \vdots & \vdots & \ddots & \vdots & \vdots \\ S_{n-1,1} & S_{n-1,2} & \cdots & S_{n-1,n-1}+s & S_{n-1,n} \\ S_{n,1} & S_{n,2} & \cdots & S_{n,n-1} & S_{n,n} \end{bmatrix} \tag{3.35}$$

The linear elastic constants s are added on the main diagonal of the spectral matrix, except for the first and last terms, since they are fixed. The application of the simple supported case, allows to write the displacement of the second node due to a harmonic force applied at the same location as

$$\mathbf{w} = \mathbf{S}^{-1}\mathbf{f} \tag{3.36}$$

3.5 Axially moving cable with periodic elastic foundation

In this section, the axially moving cable with periodic elastic foundation, Fig. 1.2(d), was developed. As all periodic models, it is also formed by identical substructures, the cells. Figure 3.9 is the representation of the entire model with a cell highlighted in red.

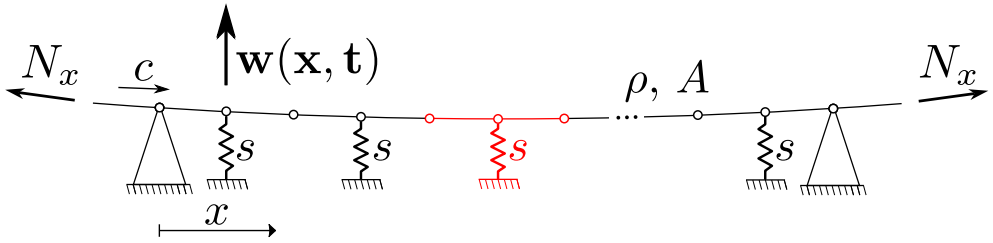

Figure 3.9: The axially moving cable with periodic elastic foundation model. The entire model is formed by the periodic cells highlighted in red. The cable is subjected to an axial force N_x, a constant moving speed c and a harmonic excitation force $\mathbf{f_2}$. The $\mathbf{w_2}$ represents the displacement of the second node.

The periodic model was developed using the SEM. The spectral matrix was transformed

into transfer matrix to analyze the periodicity.

3.5.1 Spectral Element Method

The periodic cell is detailed on Fig. 3.10 and it is composed by cell A and cell B, each one has two nodes, an axially moving cable with and elastic foundation with the linear stiffness equal to $s/2$ and the length is $L/2$. The sum $A + B$ result in the periodic cell with three nodes, an axially moving cable with and elastic foundation with the linear stiffness equal to s and the length is L The spectral matrix for cell A and cell B are given by $\mathbf{S_A}$ and $\mathbf{S_B}$.

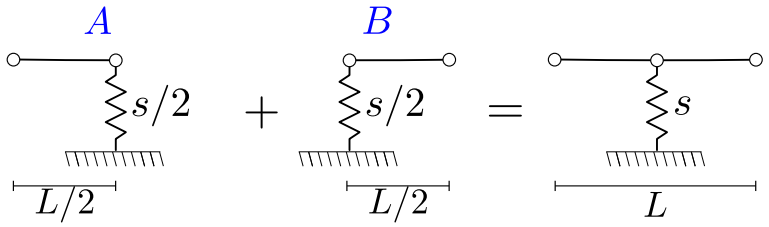

Figure 3.10: The periodic cell of the axially moving cable with periodic elastic foundation model. It is composed by cell A and cell B.

$$\mathbf{S_A} = \begin{bmatrix} S_{11} & S_{12} \\ S_{21} & S_{22} + \dfrac{s}{2} \end{bmatrix} \qquad \mathbf{S_B} = \begin{bmatrix} S_{11} + \dfrac{s}{2} & S_{12} \\ S_{21} & S_{22} \end{bmatrix} \tag{3.37}$$

The spectral matrix of the periodic cell is given by

$$\mathbf{S_{cell}} = \begin{bmatrix} S^A_{1,1} & S^A_{1,2} & 0 \\ S^A_{2,1} & S^A_{2,2} + s/2 + S^B_{1,1} + s/2 & S^B_{1,2} \\ 0 & S^B_{2,1} & S^B_{2,2} \end{bmatrix} = \begin{bmatrix} S^A_{1,1} & S^A_{1,2} & 0 \\ S^A_{2,1} & S^A_{2,2} + S^B_{1,1} + s & S^B_{1,2} \\ 0 & S^B_{2,1} & S^B_{2,2} \end{bmatrix}$$

$$\mathbf{S_{cell}} = \begin{bmatrix} S^n_{1,1} & S^n_{1,2} & S^n_{1,3} \\ S^n_{2,1} & S^n_{2,2} + s & S^n_{2,3} \\ S^n_{3,1} & S^n_{3,2} & S^n_{3,3} \end{bmatrix} \tag{3.38}$$

The periodic model with n periodic cells is showed on Fig. 3.11, since each periodic cell has three nodes, the entire model has $2n + 1$ nodes, thus the global matrix is of order $2n + 1$.

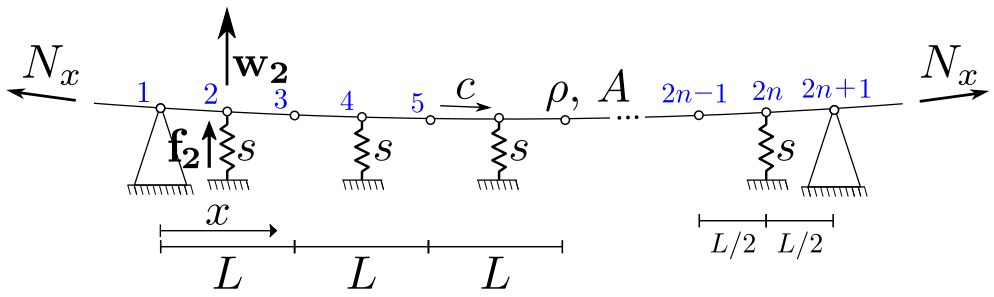

Figure 3.11: The axially moving cable with periodic elastic foundation used to develop the mathematical model. The cable is subjected to an axial force N_x, a constant moving speed c and a harmonic excitation force $\mathbf{f_2}$. The $\mathbf{w_2}$ represents the displacement of the second node.

Assembling the cell matrices $\mathbf{S_{cell}}$ on a global spectral matrix $\mathbf{S_G}$,

$$\mathbf{S_G} = \begin{bmatrix} S^1_{1,1} & S^1_{1,2} & S^1_{1,3} & 0 & 0 & \cdots & 0 & 0 & 0 \\ S^1_{2,1} & S^1_{2,2}+s & S^1_{2,3} & 0 & 0 & \cdots & 0 & 0 & 0 \\ S^1_{3,1} & S^1_{3,2} & S^1_{3,3}+S^2_{1,1} & S^2_{1,2} & S^2_{1,3} & \cdots & 0 & 0 & 0 \\ 0 & 0 & S^2_{2,1} & S^2_{2,2}+s & S^2_{2,3} & \cdots & 0 & 0 & 0 \\ 0 & 0 & S^2_{3,1} & S^2_{3,2} & S^2_{3,3}+S^3_{1,1} & \cdots & 0 & 0 & 0 \\ \vdots & \vdots & \vdots & \vdots & \vdots & \ddots & \cdots & \cdots & \cdots \\ 0 & 0 & 0 & 0 & 0 & \cdots & S^{n-1}_{3,3}+S^n_{1,1} & S^n_{1,1} & S^n_{1,1} \\ 0 & 0 & 0 & 0 & 0 & \ddots & S^n_{2,1} & S^n_{2,2}+s & S^n_{2,3} \\ 0 & 0 & 0 & 0 & 0 & \ddots & S^n_{3,1} & S^n_{3,2} & S^n_{3,3} \end{bmatrix} \tag{3.39}$$

$$\mathbf{w} = \mathbf{S}^{-1}\mathbf{f} \tag{3.40}$$

3.5.2 Transfer Matrix

The transfer matrix it is another way to show the dynamic stiffness matrix content and it relates the input forces and velocities at the output terminals. This form of description is very appropriate to describe a series of structure side by side, since the output terminals of the first is equal to the input of the second, and so on.

The properties of a complete periodic structure can be inferred from knowledge of a single

cell without requiring great computer time and cost, so the transfer matrix can be efficiently used, especially for periodic one-dimensional structures (Lee, 2000). According to Langley (1996), the eigenvalues and eigenvectors of the transfer matrix describe wave motion through the periodic system, while the eigenvectors describe the form of the wave motion while the eigenvalues are related to the change in wave amplitude across the system. Real eigenvalues correspond to decaying waves without change of phase, while complex ones correspond to decaying waves that change their phases from cell to cell (Yong and Lin, 1989).

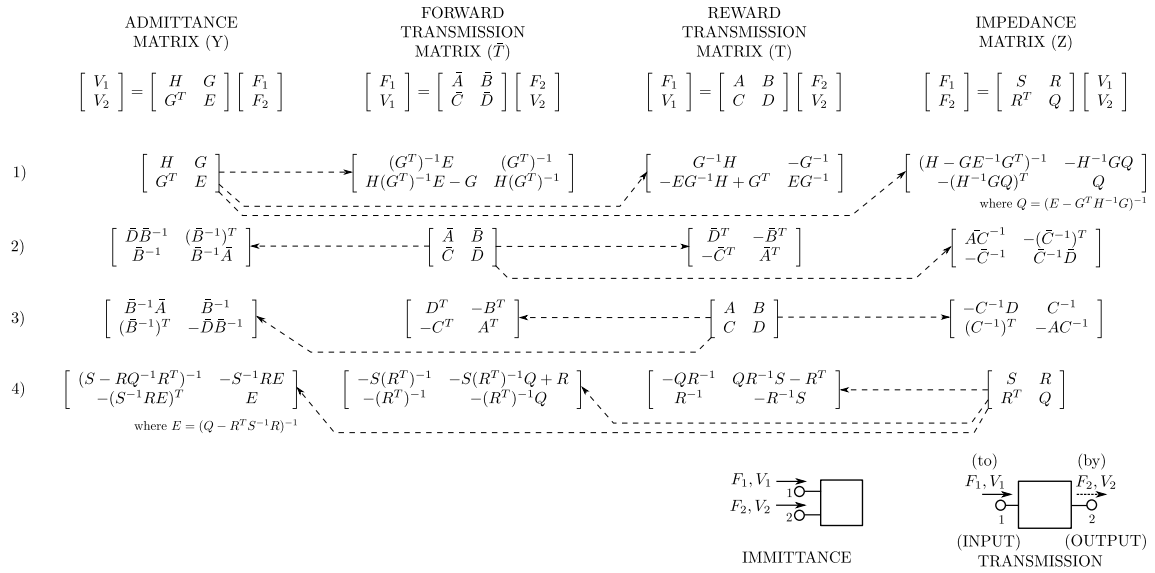

Figure 3.12: Transformations through admittance, transmission, and impedance matrices . From Rubin (1967)

Figure 3.12 shows the transformations among the admittance, transmission, and impedance matrices, according to Rubin (1967), the rows shows the transformation from the admittance, forward transmission, rearward transmission, and impedance matrices, respectively to the other column forms. The V_1 and V_2 represent the velocities or displacements of the input and output, the F_1 and F_2 are the forces on the input and output terminals of the cell.

The transformation among the spectral matrix and transmission matrix is given by Eq. 3.41, where the transfer matrix is obtained from the elements of the spectral matrix, $S_{i,j}$.

$$\mathbf{T} = \begin{bmatrix} -S_{2,2}{S_{1,2}}^{-1} & {S_{2,2}}{S_{1,2}}^{-1}S_{1,1} - S_{2,1} \\ {S_{1,2}}^{-1} & -{S_{1,2}}^{-1}S_{1,1} \end{bmatrix} \tag{3.41}$$

The spectral matrix relates the force and displacements vectors as $\mathbf{f} = \mathbf{Sw}$ and the transfer matrix relates the input and output terminals as

$$\psi_{\mathbf{2}} = \mathbf{T}\psi_{\mathbf{1}} \tag{3.42}$$

where $\psi_{\mathbf{1}} = \begin{bmatrix} F_1 & W_1 \end{bmatrix}^T$ and $\psi_{\mathbf{2}} = \begin{bmatrix} F_2 & W_2 \end{bmatrix}^T$ are the state vectors of the first and second terminals.

Applying the transformation into transfer matrix to the cells A and B of the Fig. 3.10,

$$\psi_{\mathbf{2}} = \mathbf{T_A}\psi_{\mathbf{1}} \tag{3.43}$$

$$\psi_{\mathbf{3}} = \mathbf{T_B}\psi_{\mathbf{2}} \tag{3.44}$$

$$\psi_{\mathbf{3}} = \mathbf{T_B}[\mathbf{T_A}]\psi_{\mathbf{1}} \tag{3.45}$$

$$\psi_{\mathbf{3}} = \mathbf{T}\psi_{\mathbf{1}} \tag{3.46}$$

where $\mathbf{T_A}$ and $\mathbf{T_A}$ are the transfer matrices for the A and B cells respectively, and the $\mathbf{T}$ is the transfer matrix for the periodic cell.

According to Gonçalves (2007), the wave mode propagation along a periodic structure can be defined as

$$\psi_{n+1} = \lambda\psi_n \tag{3.47}$$

which shows that the state vector of two adjacent terminals are related by a λ factor. This in addition to the transfer matrix relation from Eq. 3.46 forms an eigenvalue problem.

The parameter λ is related to the propagation constant, μ, by letting $\lambda = e^{i\mu}$. A real wave propagation constant corresponds to a wave propagating without attenuation, while an imaginary component to the propagation constant defines the band gap (Hvatov and Sorokin, 2015).

3.6 Chapter remarks

Inspired on the model proposed by Lee (2009), the simple supported model was modeled by the Spectral Element (SEM) and Finite Element (FEM) methods. The elastic foundation and the periodic elastic foundation were added using the SEM. From the periodic elastic foundation model, using SEM, and applying the transformation among impedance and transmission matrix according to Rubin (1967), the spectral matrix was transformed into transfer matrix in order to evaluate the dispersion relation of the system.

4. Numerical analysis

In this chapter, numerical analysis is performed using the models presented in the previous chapter. The system behavior is studied based on the analysis of frequency response functions (FRFs), to evaluate the effects of the moving speed and the influence of the stiffness of the elastic foundation. For the transfer matrix model, considering a range of frequency, the eigenvalue of the global transfer matrix is obtained to evaluate the influence of the speed on the propagation and attenuation regions. Each section of this chapter contains the analyses and results of each model studied.

4.1 Parametric analysis

The properties values used on the numerical simulations, showed on Tab. 4.1, were obtained from Lee (2009). All models studied have the same cable properties, ρ and A, and are subjected to the same axial tension N_x. The simple supported and the elastic foundation models has cable length, L,equal to the total length of the cable. In the periodic model, cable length, L, refers to the distance between two subsequent supports and not to the length of the entire model. Thus, as the number of cells increases, the length of the model grows. The numerical simulations results were used to evaluate the influence of the moving speed and the elastic foundation stiffness by comparing the different models. It was used a structural damping on the axial tension, N_x, using the complex Young's modulus with $E\,(1 + j\eta)$

The parameters were chosen in order to simplify the analysis and the understanding of the system dynamic behavior and do not correspond to any typical system.

Table 4.1: Properties used on the numerical simulation.

Property	**Value**
Cable length (L)	2 $[m]$
Axial tension (N_x)	10 $[kN]$
Mass per unit length (ρA)	1 $[kg/m]$
Periodic cell length (L)	2 $[m]$
Structural damping (η)	0.005

A Frequency Response Function (or FRF) is used to identify the natural frequencies of a physical structure and express the relationship between an input and output on the frequency domain. It was made to evaluate the effects of the moving speed and elastic foundation stiffness changes on the **resonant frequencies** of the models. The static system, $c = 0\, m/s$, represents the cable without moving.

4.2 Simple supported axially moving system

For the first model, showed on Fig. 4.1, the axially moving speed, c, was varied to obtain the results and a FRF was calculate for the displacement of the second node in the middle of the cable. The first and third nodes are fixed due to the supports then in the second node the force was applied and the displacement was measured. This model was analyzed using both the spectral element and the finite element methods.

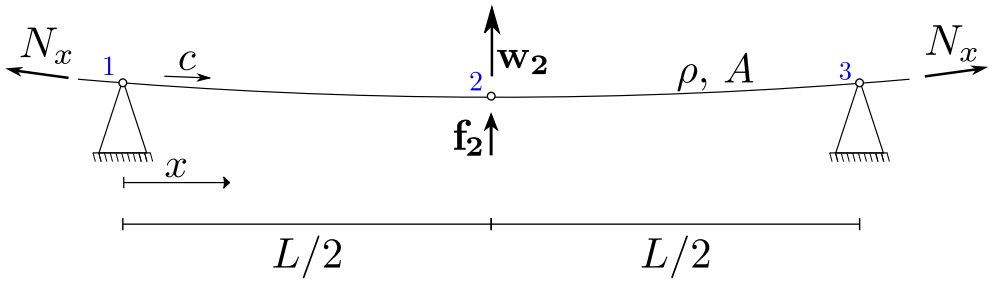

Figure 4.1: The axially moving cable with two elements model. The cable is subjected to an axial force N_x, a constant moving speed c and a harmonic excitation force $\mathbf{f}$. The $\mathbf{w_2}$ represents the displacement of the second node.

Figure 4.2 shows the moving speed influence on the resonant frequency, (a) is a top view of the FRF for a range, 0 to 100 m/s, of moving speed, the darker curves shows the resonance peaks. It was obtained using the SEM. Fig. 4.2(b) shows the FRF for three moving speed (0, 35 and 70 m/s) comparing both SEM and FEM. For the FEM model 300 elements were used.

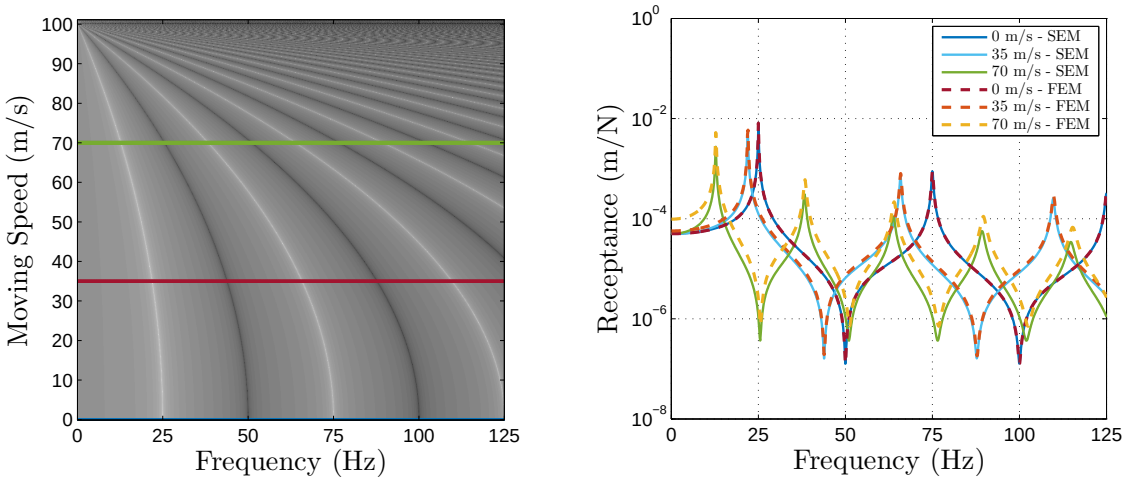

(a) (b)

Figure 4.2: FRF for the axially moving cable with simple supports (a) is the upper view of the FRF for a range of speed. The darker curves are the resonant frequencies. There are three speeds highlighted for better visualization, in blue and full line is the static system, in red and dashed line the system with moving speed $c = 35\,m/s$, and in green and dot dashed line $c = 70\,m/s$. (b) is the comparison of the three speeds highlighted.

Observing Fig. 4.2(a) it can be concluded that the increasing speed decreases all the resonant frequencies and the increasing speed also decreases the anti resonant frequencies. The critical speed of this system is 100 m/s, at this speed all the natural frequencies became zero and a static instability occurs. In Fig. 4.2(b) three moving speed are highlighted comparing

both Spectral and Finite Element Methods. As the moving speed increases, the resonance and antiresonance decreases. For 0 and $35\,m/s$ the FEM accuracy is comparable to SEM, but for $70\,m/s$, specially on high frequency, there are small numerical errors.

The chose of the finite elements number was based on numerical simulations for the four firts natural frequencies in comparison with the exact theory from Lee (2009). The results are showed on Tab.4.2.

Table 4.2: Comparison between analytical response and number of finite elements used, speed given in m/s and frequency in Hz.

Speed	**Frequency**	**Theory**	**100 elements**	**200 elements**	**300 elements**
0	f_1	25.0	25.0	25.0	25.0
	f_2	50.0	50.0	50.0	50.0
	f_3	75.0	75.0	75.0	75.0
	f_4	125.0	125.1	125.0	125.0
20	f_1	24.0	24.5	24.5	24.5
	f_2	48.0	49.0	49.0	49.0
	f_3	72.0	73.5	73.5	73.5
	f_4	120.0	122.6	122.5	122.5
50	f_1	18.7	21.7	21.7	21.6
	f_2	37.5	43.5	43.4	43.3
	f_3	56.2	65.3	65.1	65.0
	f_4	93.7	108.9	108.5	108.4

4.3 Axially moving cable with elastic foundation

For the second and third models, showed on Fig. 4.3 and Fig. 4.21 respectively, the first analyzes were made by varying the linear elastic constant, s, on the static system, $c = 0\,m/s$, the results obtained revealed the influence of the elastic foundation on the natural frequency. For the second analyses, it was fixed a value for the linear elastic constant, s, and then varied the moving speed, c.

4.3.1 Spectral Element Method

Boundary elastic foundation

The first node of this model is fixed due to the support then in the second node the force was applied and the displacement was measured.

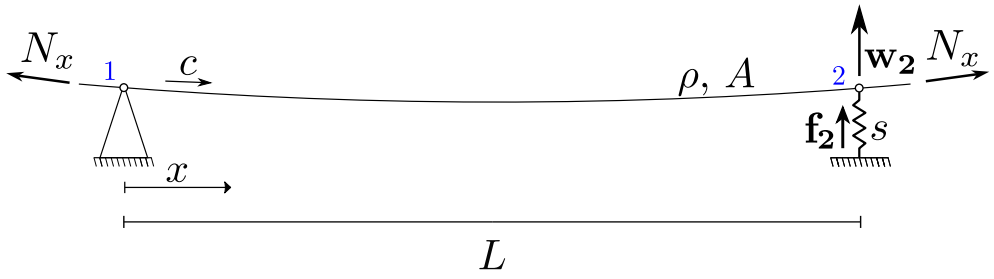

Figure 4.3: The axially moving cable with elastic foundation model. The cable is subjected to an axial force N_x, a constant moving speed c and a harmonic excitation force $\mathbf{f}$. The $\mathbf{w_2}$ represents the displacement of the second node.

Figure 4.4 shows the elastic foundation influence on the resonance, (a) is the top view of the FRF, where the lighter curves represent the resonance peak and the darker curves represent the anti-resonance.

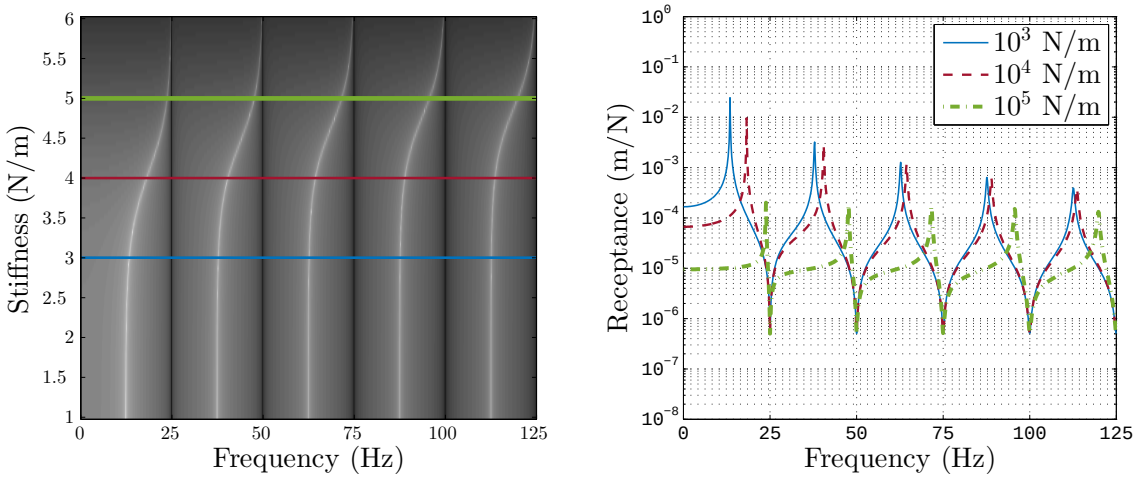

(a) (b)

Figure 4.4: FRF for the static axially moving cable with elastic foundation (a) is the upper view of the FRF for a range of stiffness of the elastic support on a log scale. The lighter curves are the resonant frequencies. There are three stiffness highlighted for better visualization, in blue and full line the stiffness is $s = 10^3\, N/m$, in red and dashed line the $s = 10^4\, N/m$, and in green and dot dashed line $s = 10^5\, N/m$. (b) is the comparison of the FRF for the three stiffness highlighted on (a).

The elastic foundation stiffness was varied between 10^1 and 10^6. The the lighter lines represent the resonance and the darker lines represent the anti-resonance. In the range between 10^1 and 10^3, the elastic foundation does not interfere in the resonance, as it does not offer resistance to movement, the lighter lines are straight. On the other hand, for elastic foundation values bigger than $10^5\, N/m$ it inhibits movement, the lighter lines overlap the darker ones. In the range between 10^3 and $10^5\, N/m$ increasing the value of s increases the natural frequency. The influence of the elastic foundation is greatest at low frequency, where the stiffness of the system has bigger influence. However, the elastic base has no influence on the anti-resonance, this can be easily seen in Fig. 4.4(a), because the darker lines are straight. From Fig. 4.4, three values of s were chosen to study the influence of speed on the model with an elastic foundation.

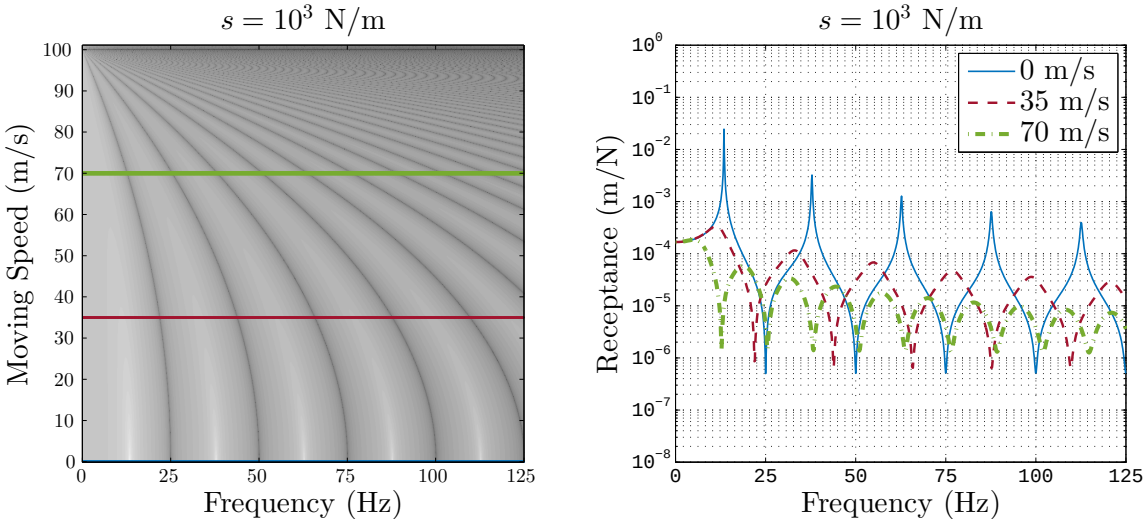

Figure 4.5: FRF for the axially moving cable with an elastic foundation of stiffness $s = 10^3\, N/m$. (a) is the upper view of the FRF for a range of speed. The darker curves are the resonant frequencies. There are three speeds highlighted for better visualization, in blue and full line is the static system, in red and dashed line the system with moving speed $c = 35\, m/s$, and in green and dot dashed line $c = 70\, m/s$. (b) is the comparison of the three speeds highlighted on (a).

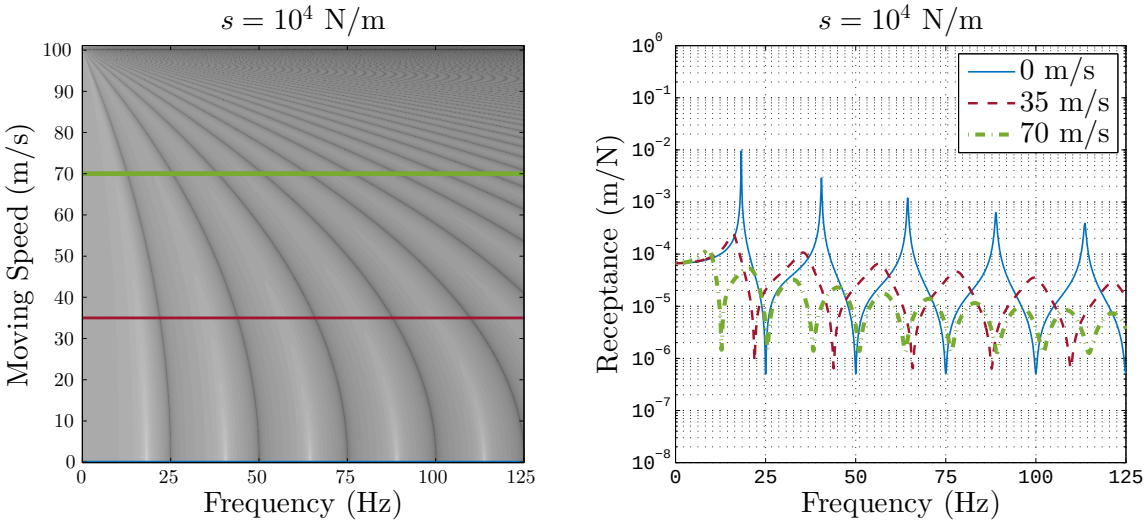

Figure 4.6: FRF for the axially moving cable with an elastic foundation of stiffness $s = 10^4\, N/m$. (a) is the upper view of the FRF for a range of speed. The darker curves are the resonant frequencies. There are three speeds highlighted for better visualization, in blue and full line is the static system, in red and dashed line the system with moving speed $c = 35\, m/s$, and in green and dot dashed line $c = 70\, m/s$. (b) is the comparison of the three speeds highlighted on (a).

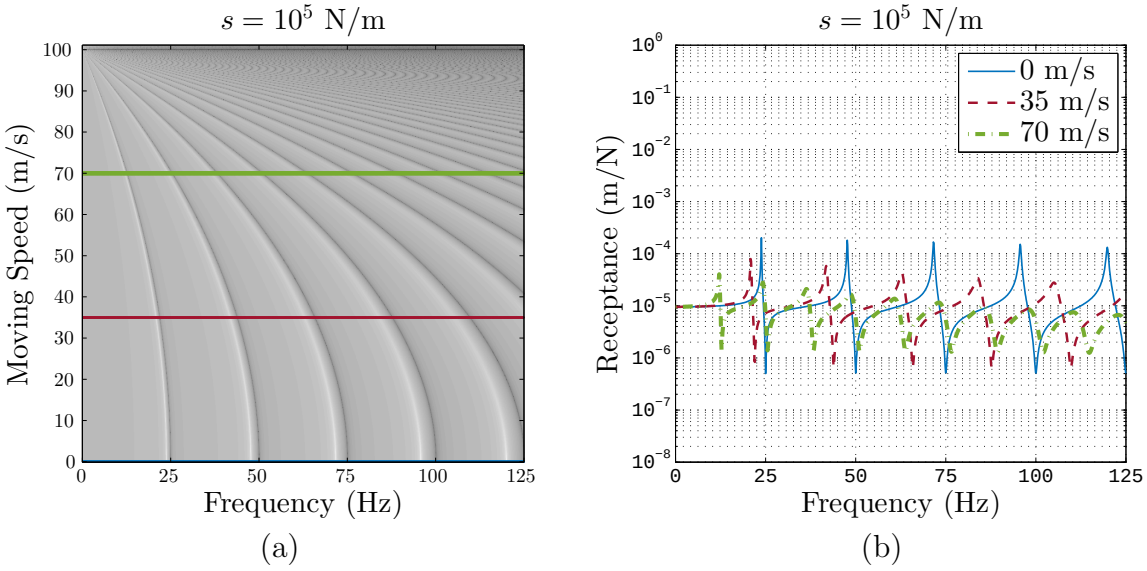

Figure 4.7: FRF for the axially moving cable with an elastic foundation of stiffness $s = 10^5\, N/m$. (a) is the upper view of the FRF for a range of speed. The darker curves are the resonant frequencies. There are three speeds highlighted for better visualization, in blue and full line is the static system, in red and dashed line the system with moving speed $c = 35\, m/s$, and in green and dot dashed line $c = 70\, m/s$. (b) is the comparison of the three speeds highlighted on (a).

Figures 4.4, 4.6 and 4.7 shows the top view of the FRF for a range of speed and also highlight three moving speed, however each Figure has a different value stiffness. Figure 4.5: $s = 10^3\, N/m$, Fig. 4.6: $s = 10^4\, N/m$ and Fig. 4.7: $s = 10^5\, N/m$. The influence of the speed is the same as in the simple supported model, increasing speed decreases the natural frequencies. In this model however a damping effect appears with increasing speed, such damping is best expressed at high frequency and with lower values of s, a fact that is better seen in Fig. 4.7.

It also can be seen that the critical speed is not related with the elastic foundation. The critical speed is $100\, m/s$ for both the simple supported model and the boundary elastic foundation configuration.

The boundary conditions of this model are the simple suport in one end, Eq. 4.1, and the the elastic foundation in the other end, Eq. 4.2. This difference on the boundary conditions explains the damping on the results. The simple support does not allow the cable to move on its transversal direction, which is the same direction that the displacement results were

obtained, the elastic foundation boundary allows the cable to move.

$$N_x w^{'}(0) = 0 \tag{4.1}$$

$$N_x w^{'}(L) = sw(L) \tag{4.2}$$

Middle span elastic foundation

Four elements were used in order to have the cable response at positions in between the node where the spring is attached and the boundaries. The first and fifth nodes of this model are fixed due to the supports, the force was applied on the third node and the displacement was measured on the third and fourth nodes.

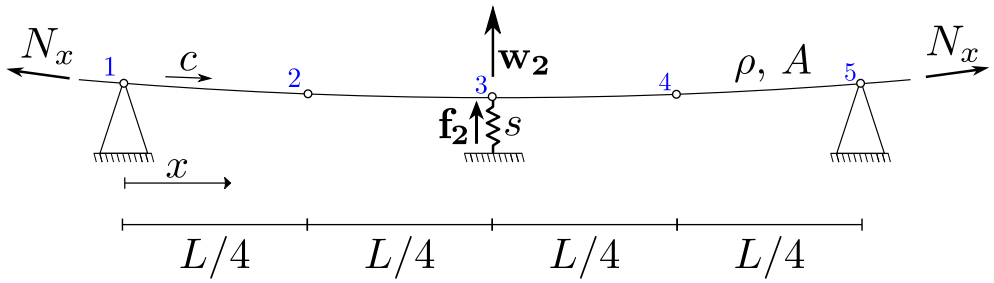

Figure 4.8: The axially moving cable with elastic foundation model. The cable is subjected to an axial force N_x, a constant moving speed c and a harmonic excitation force $\mathbf{f}$. The $\mathbf{w_2}$ represents the displacement of the second node.

First the results for the displacement of the third node, the middle of the cable. For the static cable and varying the stiffness, Fig. 4.9 shows the upper view of the FRF on log scale and three stiffness values emphasized. The elastic foundation increases the resonance frequency and do not interfere in the anti resonance frequency.

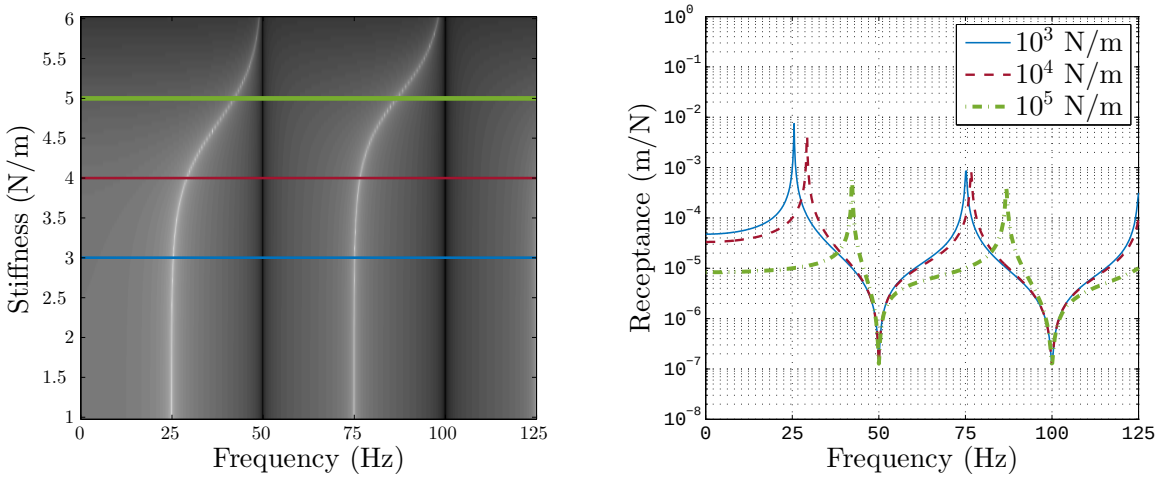

(a) (b)

Figure 4.9: On the third node FRF for the static axially moving cable with elastic foundation (a) is the upper view of the FRF for a range of stiffness of the elastic support on a log scale. The lighter curves are the resonant frequencies. There are three stiffness highlighted for better visualization, in blue and full line the stiffness is $s = 10^3\, N/m$, in red and dashed line the $s = 10^4\, N/m$, and in green and dot dashed line $s = 10^5\, N/m$. (b) is the comparison of the FRF for the three stiffness highlighted on (a).

The elastic foundation stiffness was varied between 10^1 and $10^6\, N/m$. The the lighter lines represent the resonance and the darker lines represent the anti-resonance. The influence of the elastic foundation in this configuration is similar to the boundary elastic foundation. As well as the previous configuration, in the range between 10^1 and $10^3\, N/m$, the elastic foundation does not interfere in the resonance, the lighter lines are straight. For elastic foundation values bigger than $10^6\, N/m$ it inhibits movement, the lighter lines intersect with dark ones. In the range between 10^3 and $10^6\, N/m$ increasing the value of s increases the natural frequency. The influence of the elastic foundation is also greatest at low frequency, where the stiffness of the system has bigger influence. Along with the boundary elastic foundation configuration, the elastic base has no influence on the anti-resonance, this can be easily seen in Fig. 4.9(a), because the darker lines are straight.

Choosing three values for the spring stiffness, the subsequent figures shows the FRF varying the speed for each stiffness. Comparing with the static system, the increasing speed in the presence of the elastic foundation decreases the resonance frequencies and also decreases the anti resonance frequencies, for the three models observed.

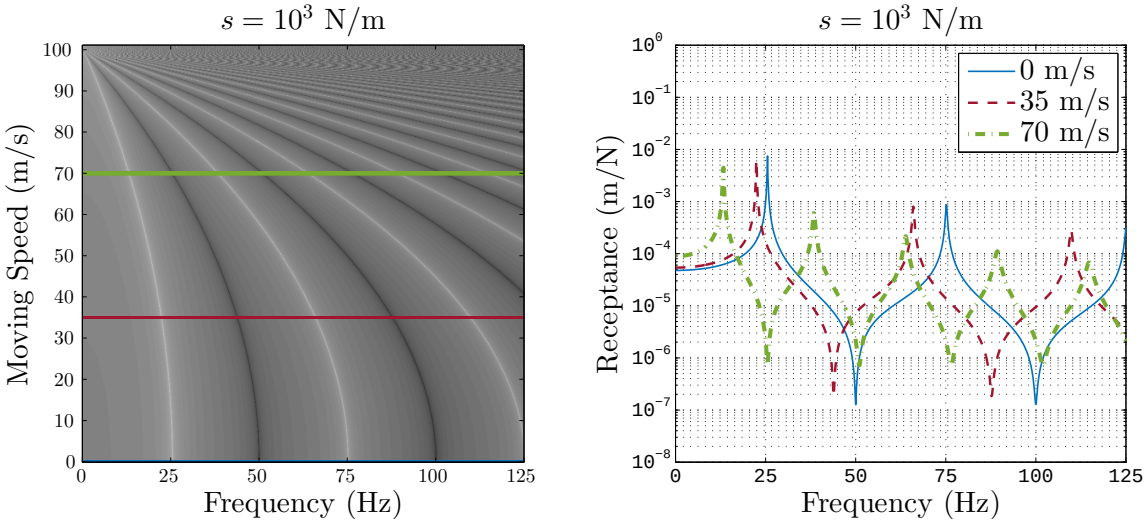

Figure 4.10: On the third node FRF for the axially moving cable with an elastic foundation of stiffness $s = 10^3\, N/m$. (a) is the upper view of the FRF for a range of speed. The darker curves are the resonant frequencies. There are three speeds highlighted for better visualization, in blue and full line is the static system, in red and dashed line the system with moving speed $c = 35\, m/s$, and in green and dot dashed line $c = 70\, m/s$. (b) is the comparison of the three speeds highlighted on (a).

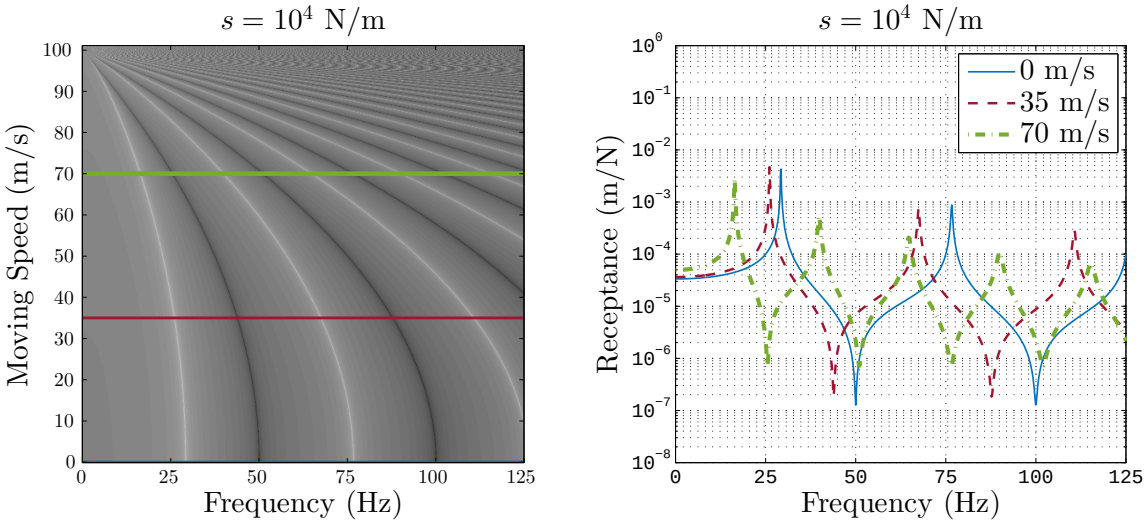

Figure 4.11: On the third node FRF for the axially moving cable with an elastic foundation of stiffness $s = 10^4\, N/m$. (a) is the upper view of the FRF for a range of speed. The darker curves are the resonant frequencies. There are three speeds highlighted for better visualization, in blue and full line is the static system, in red and dashed line the system with moving speed $c = 35\, m/s$, and in green and dot dashed line $c = 70\, m/s$. (b) is the comparison of the three speeds highlighted on (a).

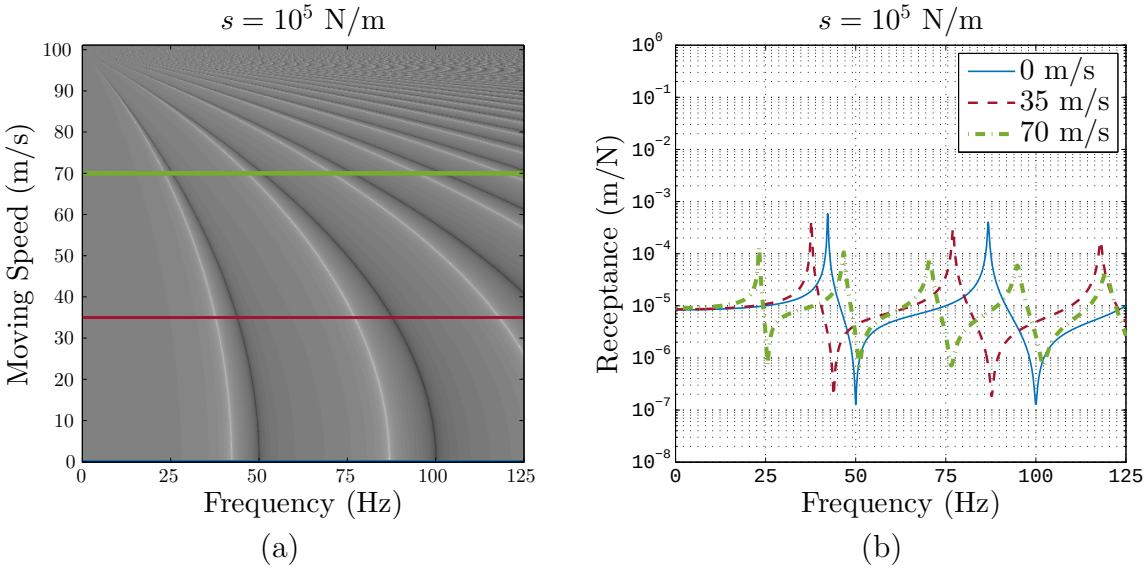

Figure 4.12: On the third node FRF for the axially moving cable with an elastic foundation of stiffness $s = 10^5\, N/m$. (a) is the upper view of the FRF for a range of speed. The darker curves are the resonant frequencies. There are three speeds highlighted for better visualization, in blue and full line is the static system, in red and dashed line the system with moving speed $c = 35\, m/s$, and in green and dot dashed line $c = 70\, m/s$. (b) is the comparison of the three speeds highlighted on (a).

With the increase of the spring stiffness the difference between the resonance and the anti resonance frequencies is smaller, this means that the system present a smaller frequency region with high displacement amplitude.

The results for the displacement in the fourth node, between the node where the spring is attached and the boundaries, are very similar to the results for the middle of the cable, except that there is no anti-resonance between the first and second resonance peak.

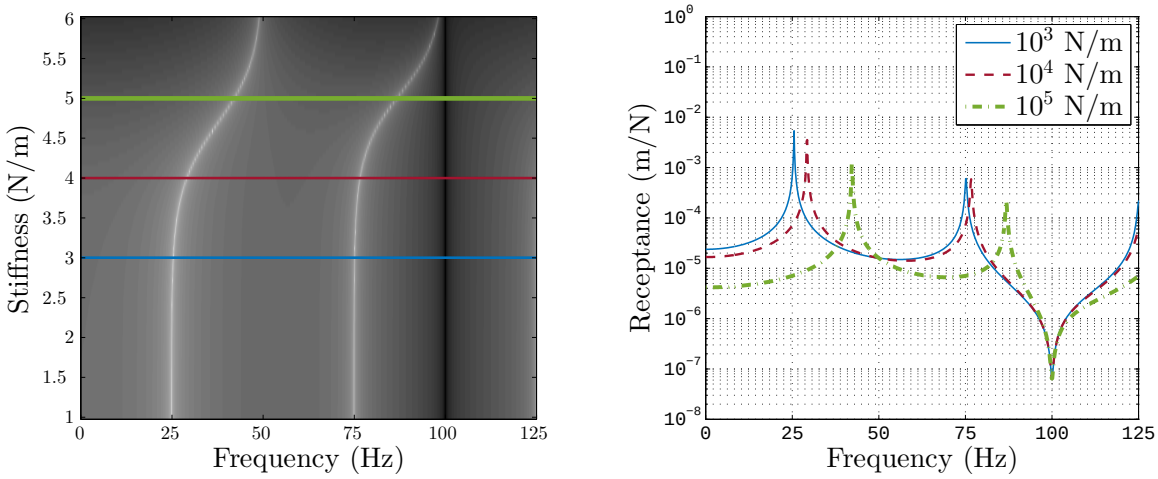

(a) (b)

Figure 4.13: On the fourth node FRF for the static axially moving cable with elastic foundation (a) is the upper view of the FRF for a range of stiffness of the elastic support on a log scale. The lighter curves are the resonant frequencies. There are three stiffness highlighted for better visualization, in blue and full line the stiffness is $s = 10^3\, N/m$, in red and dashed line the $s = 10^4\, N/m$, and in green and dot dashed line $s = 10^5\, N/m$. (b) is the comparison of the FRF for the three stiffness highlighted on (a).

The elastic foundation influence on the natural frequencies is in the range between $10^3\, N/m$ and $10^6\, N/m$, where the lighter lines vary in frequency. From 10^1 to $10^3\, N/m$ the lighter lines are straight, meaning that the resonance frequency are constant for varying the elastic foundation stiffness. Upper to $10^6\, N/m$ the resonance match the anti resonance frequency.

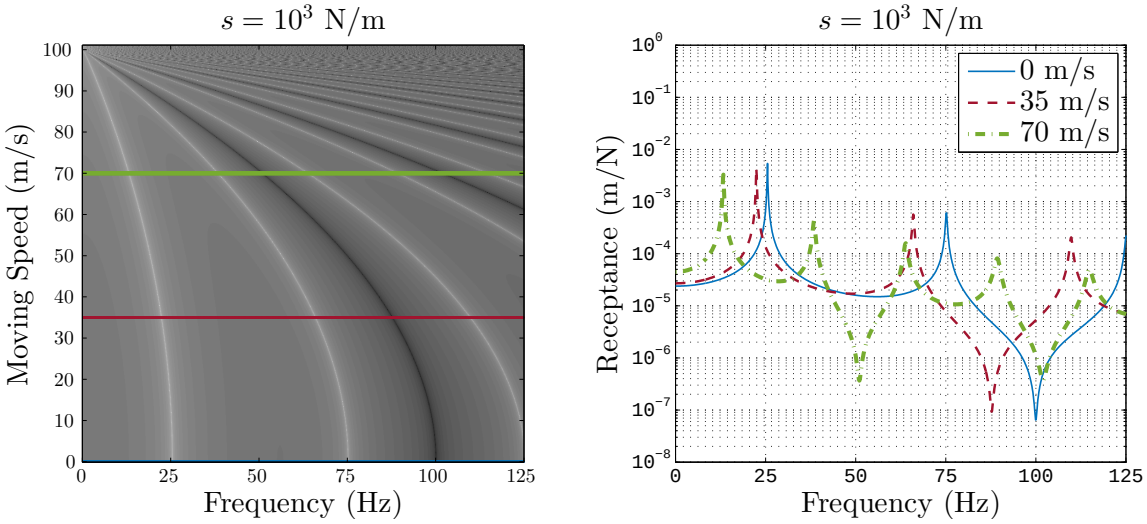

Figure 4.14: On the fourth node FRF for the axially moving cable with an elastic foundation of stiffness $s = 10^3\,N/m$. (a) is the upper view of the FRF for a range of speed. The darker curves are the resonant frequencies. There are three speeds highlighted for better visualization, in blue and full line is the static system, in red and dashed line the system with moving speed $c = 35\,m/s$, and in green and dot dashed line $c = 70\,m/s$. (b) is the comparison of the three speeds highlighted on (a).

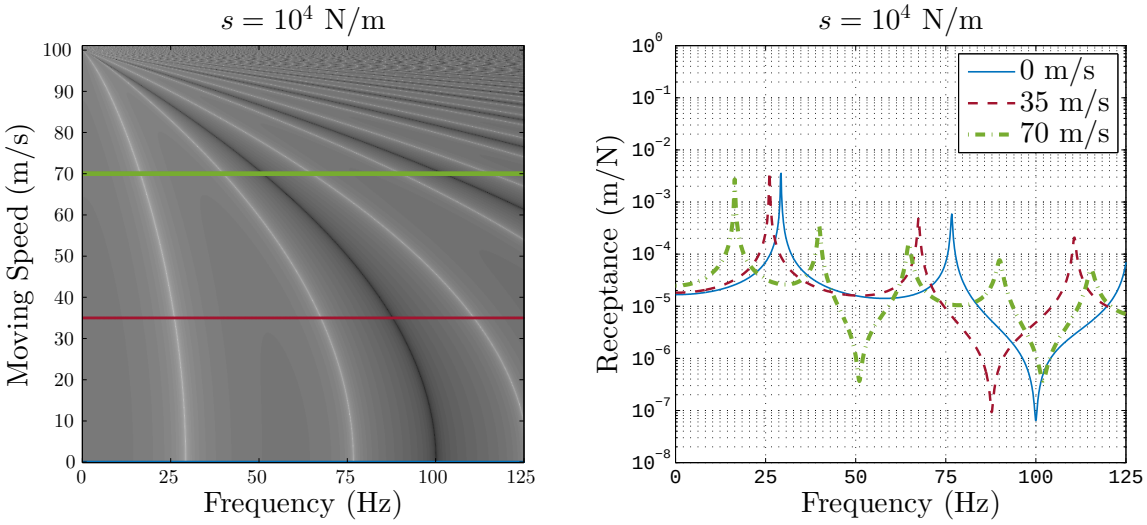

Figure 4.15: On the fourth node FRF for the axially moving cable with an elastic foundation of stiffness $s = 10^4\,N/m$. (a) is the upper view of the FRF for a range of speed. The darker curves are the resonant frequencies. There are three speeds highlighted for better visualization, in blue and full line is the static system, in red and dashed line the system with moving speed $c = 35\,m/s$, and in green and dot dashed line $c = 70\,m/s$. (b) is the comparison of the three speeds highlighted on (a).

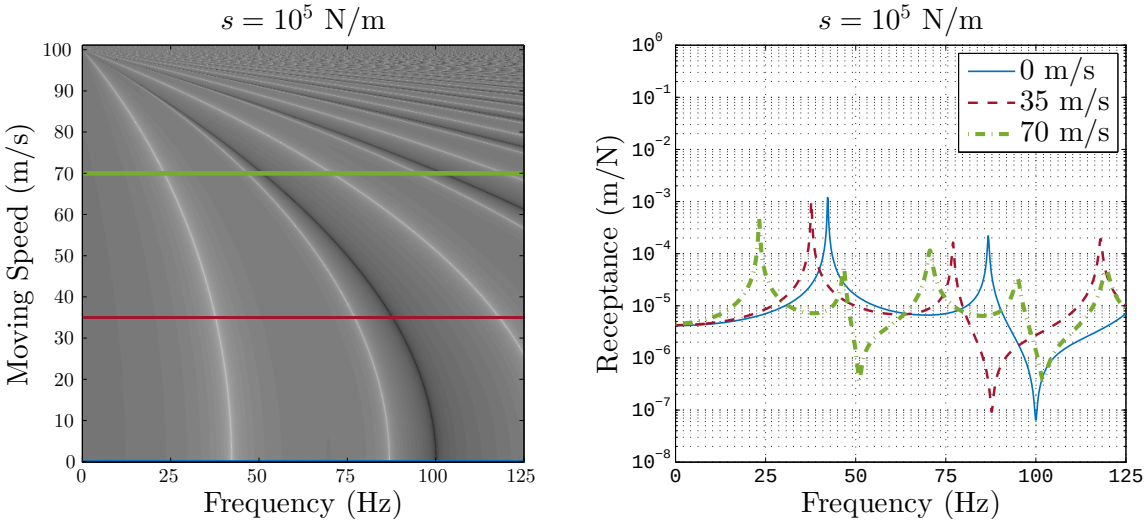

Figure 4.16: On the fourth node FRF for the axially moving cable with an elastic foundation of stiffness $s = 10^5\,N/m$. (a) is the upper view of the FRF for a range of speed. The darker curves are the resonant frequencies. There are three speeds highlighted for better visualization, in blue and full line is the static system, in red and dashed line the system with moving speed $c = 35\,m/s$, and in green and dot dashed line $c = 70\,m/s$. (b) is the comparison of the three speeds highlighted on (a).

The moving speed increase, as well as the previous configurations, decreases the resonance and antiresonance frequencies and the critical speed is $100\,m/s$ as well.

4.4 Preliminary axially moving cable with periodic elastic foundation

Numerical simulations were performed on the preliminary axially moving cable with periodic elastic foundation and the results obtained are shown as follows.

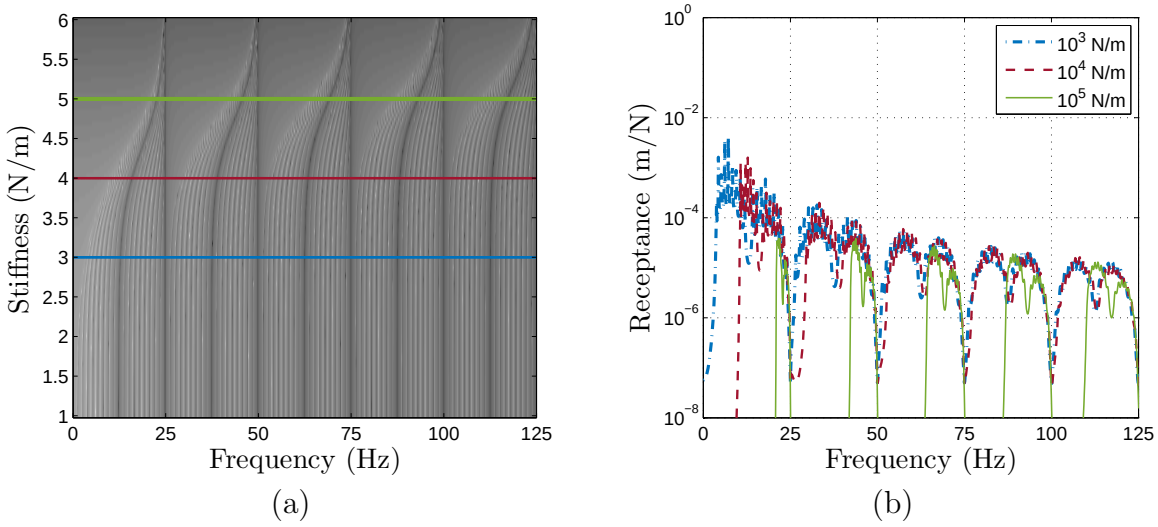

Figure 4.17: FRF for the static axially moving cable with periodic elastic foundation (a) is the upper view of the FRF for the axially moving cable with periodic elastic foundation for a range of stiffness of the elastic support on a log scale. The striped regions are propagation regions and the gray regions are the attenuation regions. (b) Three stiffness are highlighted for better visualization: in blue and full line the stiffness is $s = 10^3\, N/m$, in red and dashed line the $s = 10^4\, N/m$, and in green and dot dashed line $s = 10^5\, N/m$.

In Fig. 4.17(a), the striped regions represent the propagation zones and the whites lines of these regions are the resonance peaks. The gray regions represent the attenuation zones. Observing this figure it is possible to conclude that the linear elastic stiffness behavior in this periodic elastic foundation configuration is similar to the elastic foundation. In the range from 10^1 to $10^3\, N/m$ the resonance frequency are constant for varying the elastic foundation stiffness. Upper to $10^6\, N/m$ the resonance match the anti resonance frequency so the system seems to be fixed. In the range between 10^3 and $10^6\, N/m$ increasing linear elastic constant increases the value of natural frequencies and also decreases the propagation range as a result of the increase in the band gap regions. The propagation range decrease can also be seen in Fig. 4.17(b). The blue and dot dashed line represent the linear stiffness $10^3\, N/m$, the red and dashed line is for $10^4\, N/m$ and the full green line is for $10^5\, N/m$. The frequency region where the propagation occurs became smaller as the linear stiffness is increased. There is also a decrease of amplitude for the static system. The effects of the moving speed on the periodic elastic foundation model are shown on figures below, for three different values of s and different values of the moving speed also.

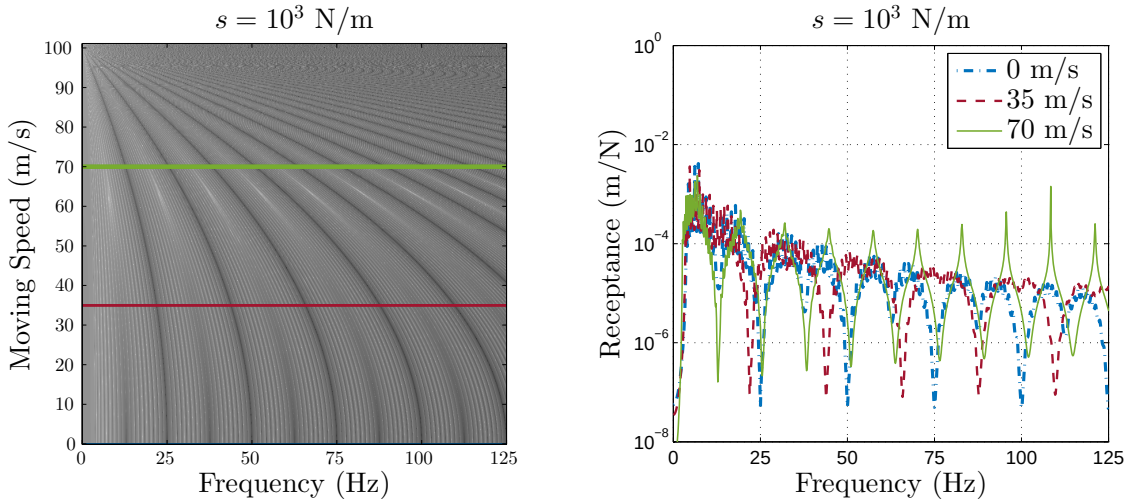

Figure 4.18: FRF for the axially moving cable with an periodic elastic foundation of stiffness $s = 10^3\, N/m$. (a) is the upper view of the FRF for a range of speed. The striped regions are propagation regions and the gray regions are the attenuation regions. (b) There are three speeds highlighted for better visualization: in blue and dot dashed line is the static system, in red and dashed line the system with moving speed $c = 35\, m/s$, and in green and full line $c = 70\, m/s$.

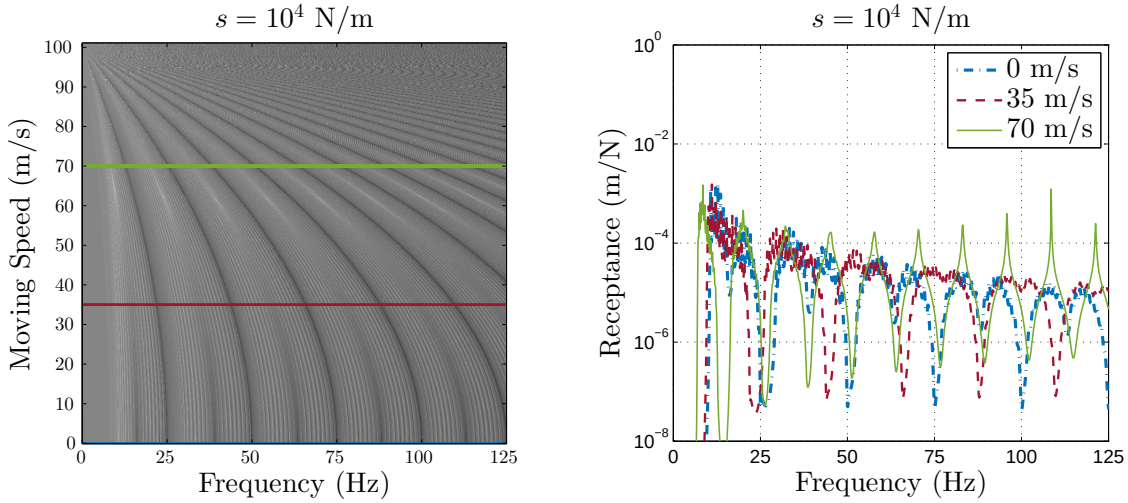

Figure 4.19: FRF for the axially moving cable with an periodic elastic foundation of stiffness $s = 10^4\, N/m$. (a) is the upper view of the FRF for a range of speed. The striped regions are propagation regions and the gray regions are the attenuation regions. (b) There are three speeds highlighted for better visualization: in blue and dot dashed line is the static system, in red and dashed line the system with moving speed $c = 35\, m/s$, and in green and full line $c = 70\, m/s$.

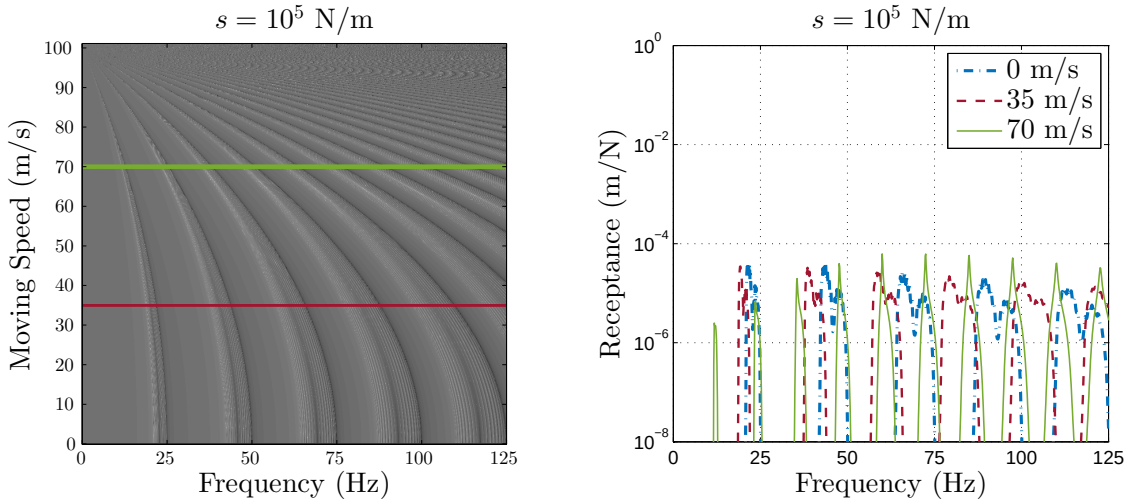

Figure 4.20: FRF for the axially moving cable with an periodic elastic foundation of stiffness $s = 10^5\, N/m$. (a) is the upper view of the FRF for a range of speed. The striped regions are propagation regions and the gray regions are the attenuation regions. (b) There are three speeds highlighted for better visualization: in blue and dot dashed line is the static system, in red and dashed line the system with moving speed $c = 35\, m/s$, and in green and full line $c = 70\, m/s$.

Figures 4.18, 4.19 and 4.20 shows the top view of the FRF for a range of speed and also shows the FRF for three moving speed (0, 35 and $70\, m/s$) with the linear elastic constant $s = 10^3\, N/m$, $s = 10^4\, N/m$ and $s = 10^5\, N/m$ respectively. In Fig. 4.18 (a), 4.19(a) and 4.20(a) the striped regions represent the propagation zones and the gray regions represent the attenuation zones.

It is important to note that even with periodic elastic foundation, independent of the linear elastic constant value, the critical speed remained $100\, m/s$. The increasing in speed decreases the natural frequency of the propagation region and makes the region narrower. In Fig. 4.18 (b), 4.19(b) and 4.20(b)are highlighted three moving speeds for each linear elastic constant, it can be seen that band gaps frequency regions start to increase as the speed increases.

4.5 Axially moving cable with periodic elastic foundation

This model was analyzed using the Spectral Element Method and then transformed into transfer matrix to analyze the wavenumbers. For the spectral element model, was varied the linear elastic constant of the periodic elastic foundation for the static system. After that, choosing three values for the linear elastic constant, was varied the moving speed of the models. For the transfer matrix model, the linear elastic constant was fixed in $s = 10^4\, N/m$ and the dispersion curves were obtained varying the moving speed.

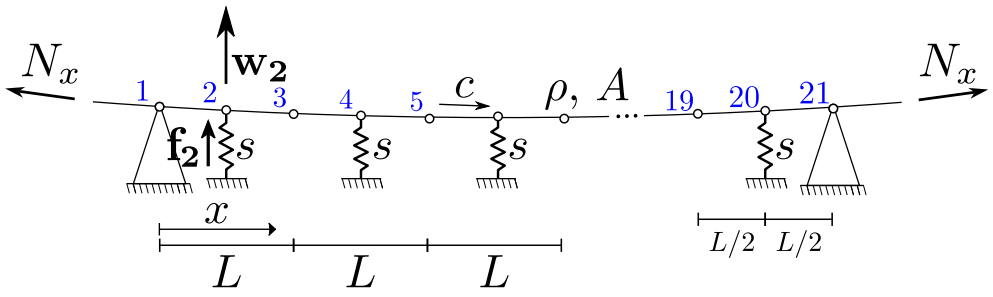

Figure 4.21: The axially moving cable with periodic elastic foundation model. The cable is subjected to an axial force N_x, a constant moving speed c and a harmonic excitation force $\mathbf{f}$. The $\mathbf{w_2}$ represents the displacement of the second node.

4.5.1 Spectral Element Method

The spectral element periodic model was analyzed with 20 cells, since each periodic cell is $2\,m$ length, the periodic model grows in size with the increase in the number of cells. Thus, the entire model is $40\,m$. The results obtained are shown as follows.

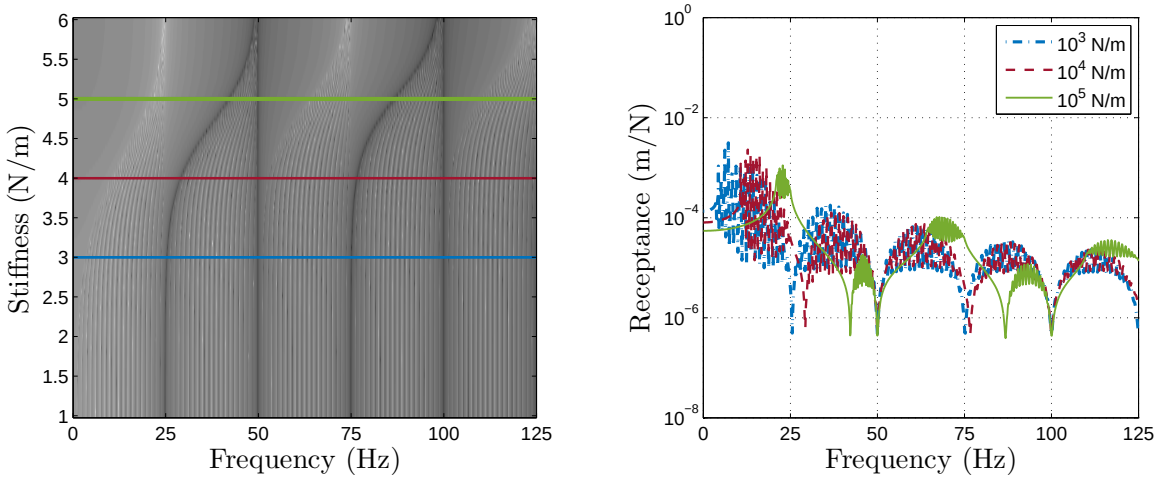

(a) (b)

Figure 4.22: FRF for the static axially moving cable with periodic elastic foundation (a) is the upper view of the FRF for the axially moving cable with periodic elastic foundation for a range of stiffness of the elastic support on a log scale. The striped regions are propagation regions and the gray regions are the attenuation regions. (b) There are three stiffness highlighted for better visualization: in blue and dot dashed line the stiffness is $s = 10^3\, N/m$, in red and dashed line the $s = 10^4\, N/m$, and in green and full line $s = 10^5\, N/m$.

Figure 4.22(a) shows the linear elastic constant variation from 10^1 to $10^6\, N/m$. The striped regions represent the propagation frequencies and the gray regions represent the attenuation frequencies. Between 10^3 and $10^6\, N/m$ a increase in the attenuation frequencies is due to the increase in the linear elastic constant. Before $10^3\, N/m$ and after $10^6\, N/m$, the influence of the elastic foundation is negligible.

Figure 4.22(b) highlight three linear elastic constant values, in blue and dot dashed line the stiffness is $s = 10^3\, N/m$, in red and dashed line the $s = 10^4\, N/m$, and in green and full line $s = 10^5\, N/m$, the increase of the linear elastic constant decreases the frequency propagation region. The effects of the moving speed on the periodic elastic foundation model are shown on figures below, for three different values of s and different values of the moving speed also.

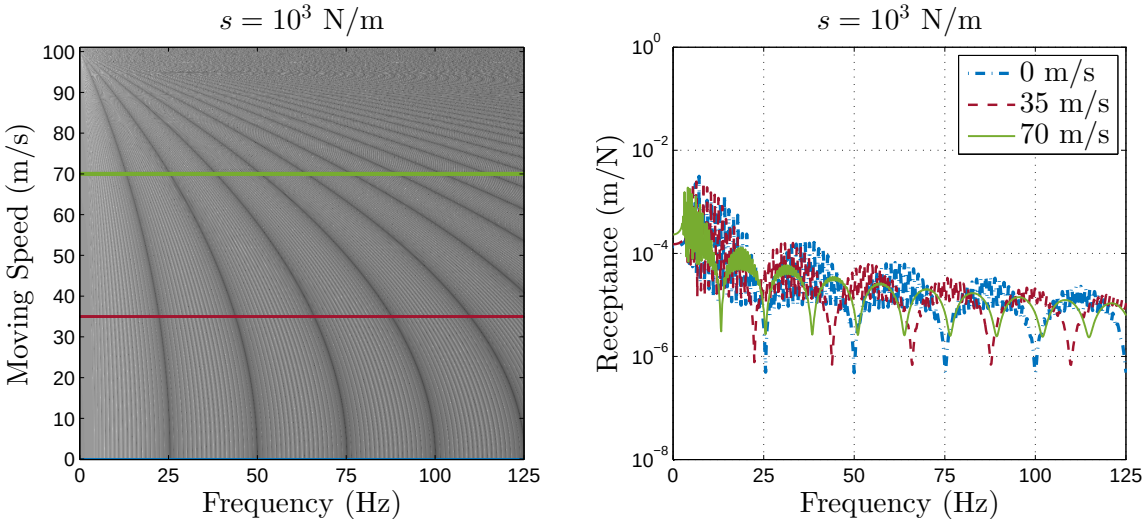

(a) (b)

Figure 4.23: FRF for the axially moving cable with an periodic elastic foundation of stiffness $s = 10^3\, N/m$. (a) is the upper view of the FRF for a range of speed. The striped regions are propagation regions and the gray regions are the attenuation regions. There are three speeds highlighted for better visualization: (a) in blue and full line is the static system, (b) in red and dashed line the system with moving speed $c = 35\, m/s$, and (c) in green and dot dashed line $c = 70\, m/s$.

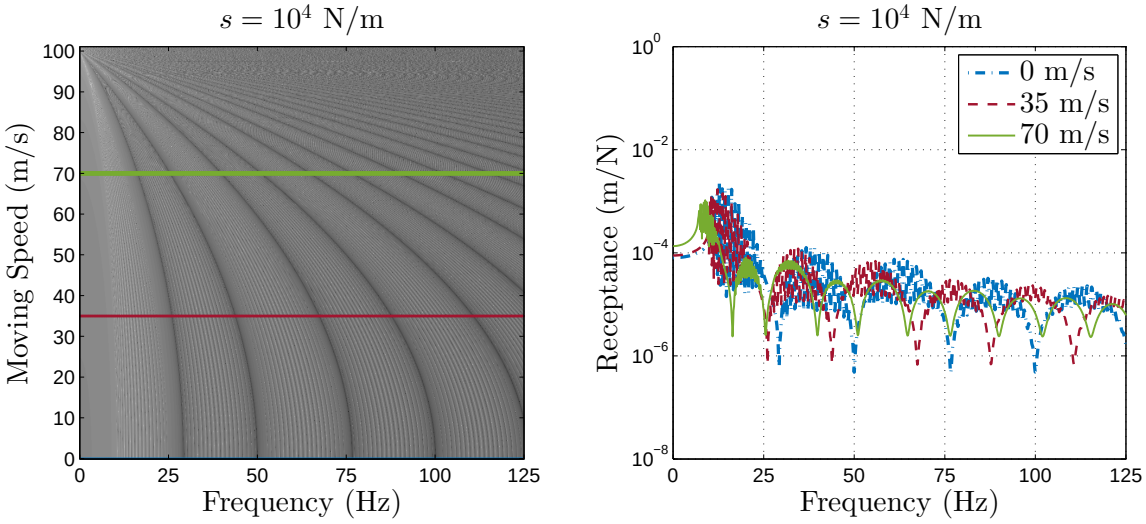

(a) (b)

Figure 4.24: FRF for the axially moving cable with an periodic elastic foundation of stiffness $s = 10^4\, N/m$. (a) is the upper view of the FRF for a range of speed. The striped regions are propagation regions and the gray regions are the attenuation regions. (b) There are three speeds highlighted for better visualization: in blue and dot dashed line is the static system, in red and dashed line the system with moving speed $c = 35\, m/s$, and in green and full line $c = 70\, m/s$.

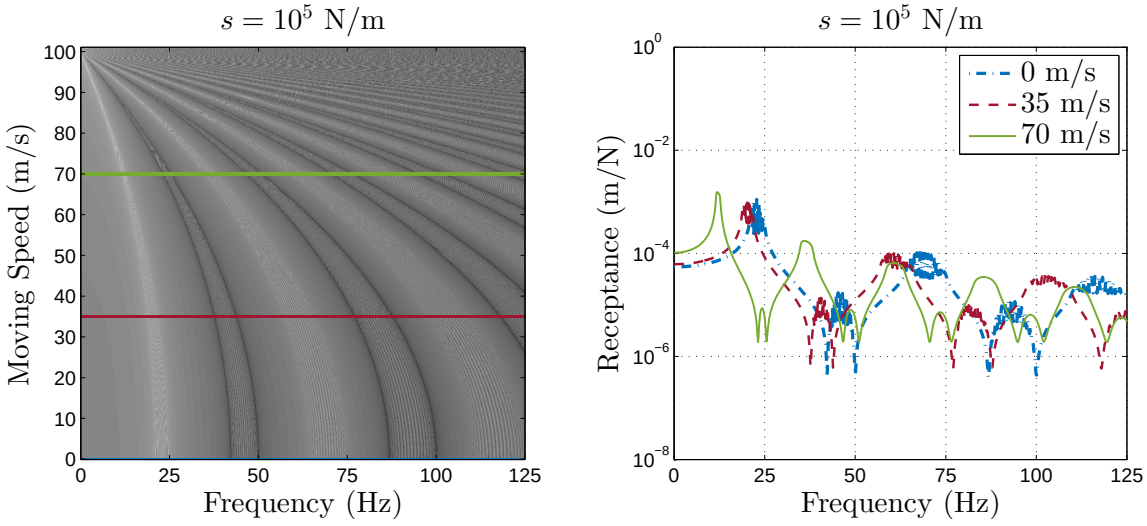

Figure 4.25: FRF for the axially moving cable with an periodic elastic foundation of stiffness $s = 10^5\, N/m$. (a) is the upper view of the FRF for a range of speed. The striped regions are propagation regions and the gray regions are the attenuation regions. There are three speeds highlighted for better visualization: (a) in blue and full line is the static system, (b) in red and dashed line the system with moving speed $c = 35\, m/s$, and (c) in green and dot dashed line $c = 70\, m/s$.

Figures 4.23, 4.24 and 4.25 shows the top view of the FRF for a range of speed and also shows the FRF for three moving speed (0, 35 and $70\, m/s$) with the linear elastic constant $s = 10^3\, N/m$, $s = 10^4\, N/m$ and $s = 10^5\, N/m$ respectively. The striped regions in Fig. 4.23 (a), 4.24(a) and 4.25(a) represent the propagation zones and the gray regions represent the attenuation zones.

The critical speed for this configuration is also $100\, m/s$, independent of the linear stiffness value. The increasing in speed decreases the frequencies of the propagation regions and makes them narrower. Observing Fig. 4.23, 4.24 and 4.25 (b) the propagation frequency zones get narrower according to the increase of the speed and the band gaps occur more frequently with increasing speed.

4.5.2 Transfer Matrix

For this model, the dispersion curves were obtained using just one periodic cell, varying the moving speed with the linear elastic constant in the values $s = 10^3\, N/m$, $s = 10^4\, N/m$ and $s = 10^5\, N/m$.

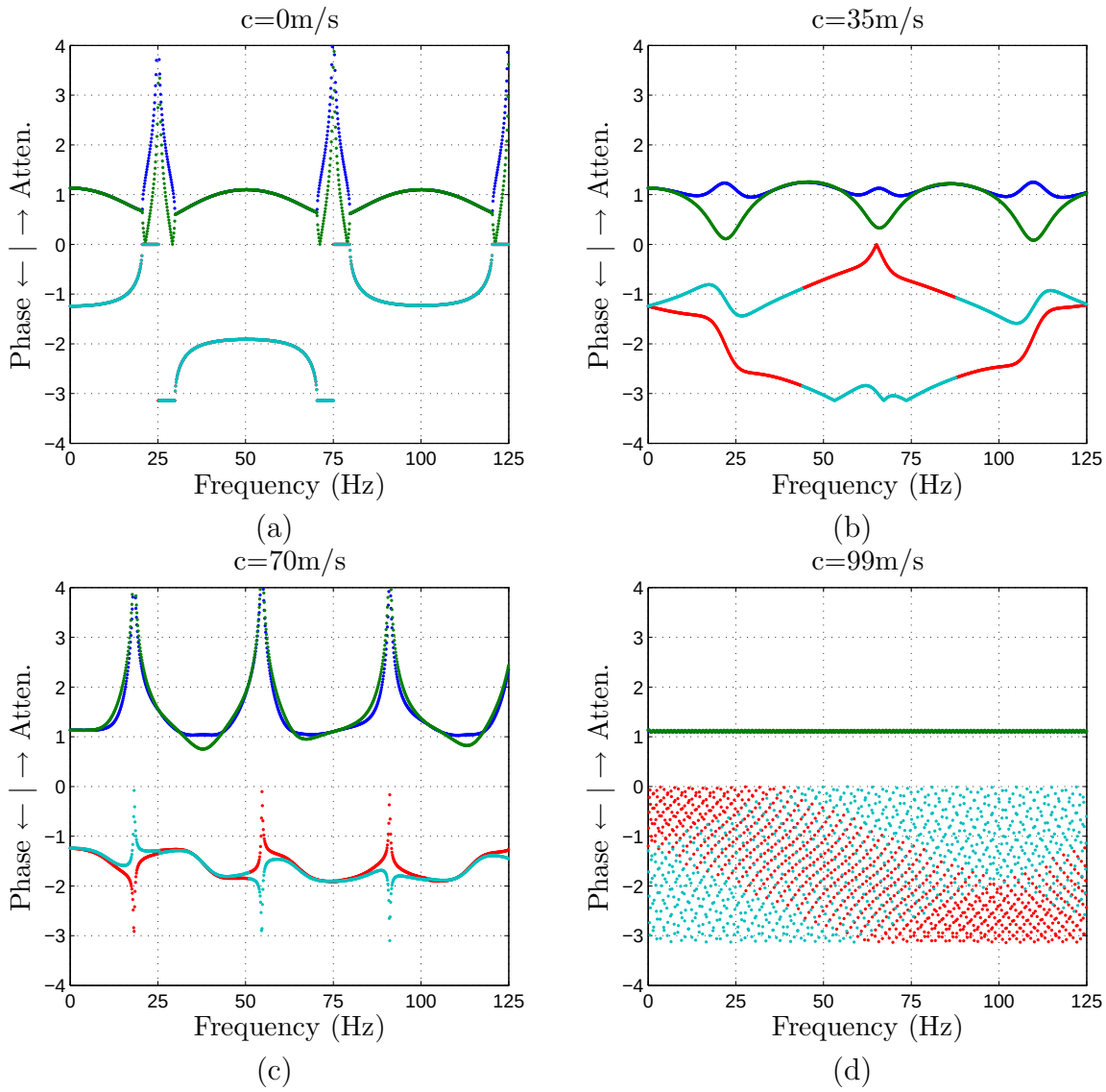

Figure 4.26: Dispersion curves for the periodic cell of the axially moving cable with periodic elastic supports with linear elastic constant $s = 10^3\, N/m$ varying the moving speed (a) the static system ($c = 0\, m/s$), (b) $c = 35\, m/s$, (c) $c = 70\, m/s$ and (d) $c = 99\, m/s$

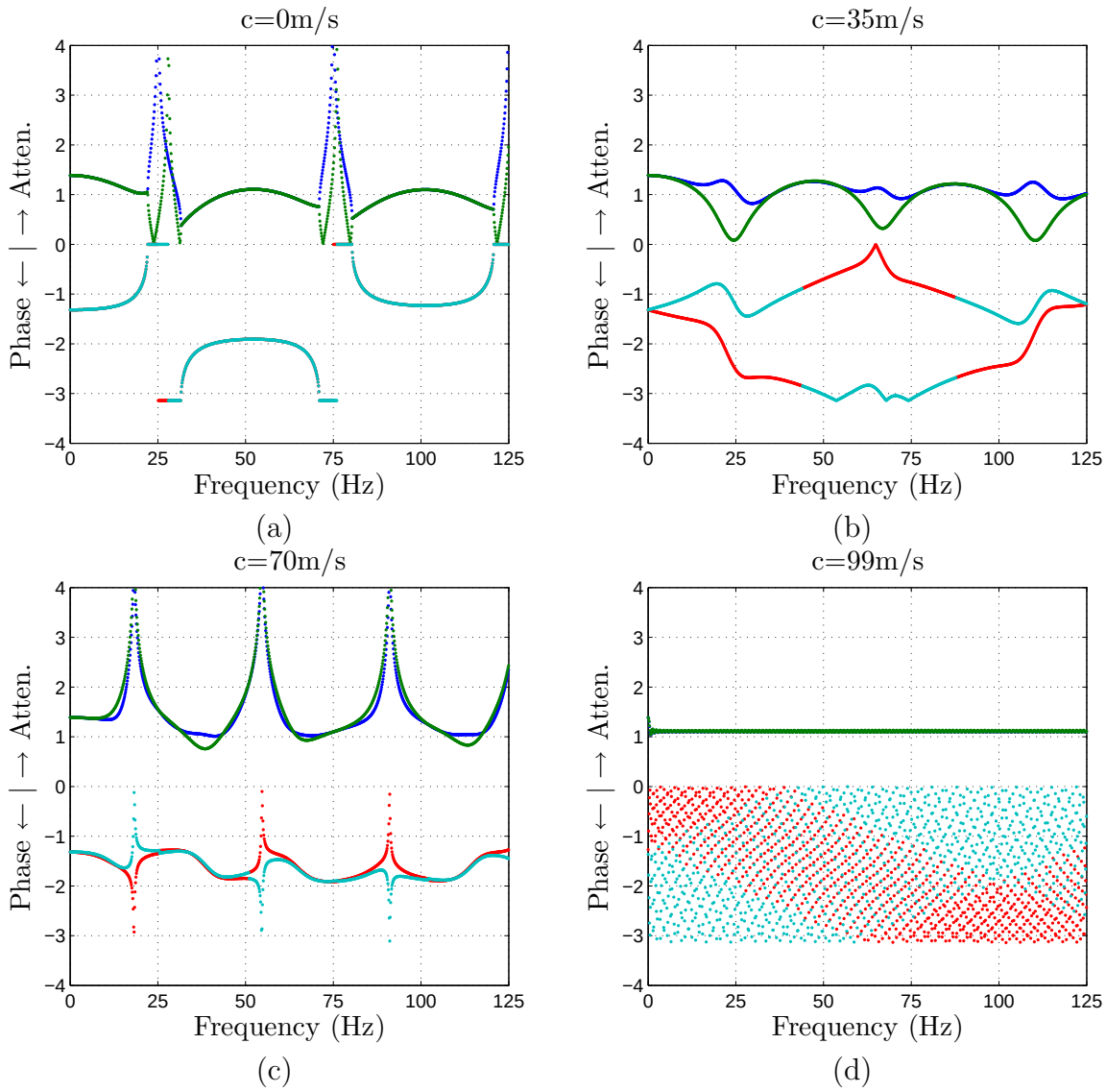

Figure 4.27: Dispersion curves for the periodic cell of the axially moving cable with periodic elastic supports with linear elastic constant $s = 10^4\, N/m$ varying the moving speed (a) the static system ($c = 0\, m/s$), (b) $c = 35\, m/s$, (c) $c = 70\, m/s$ and (d) $c = 99\, m/s$

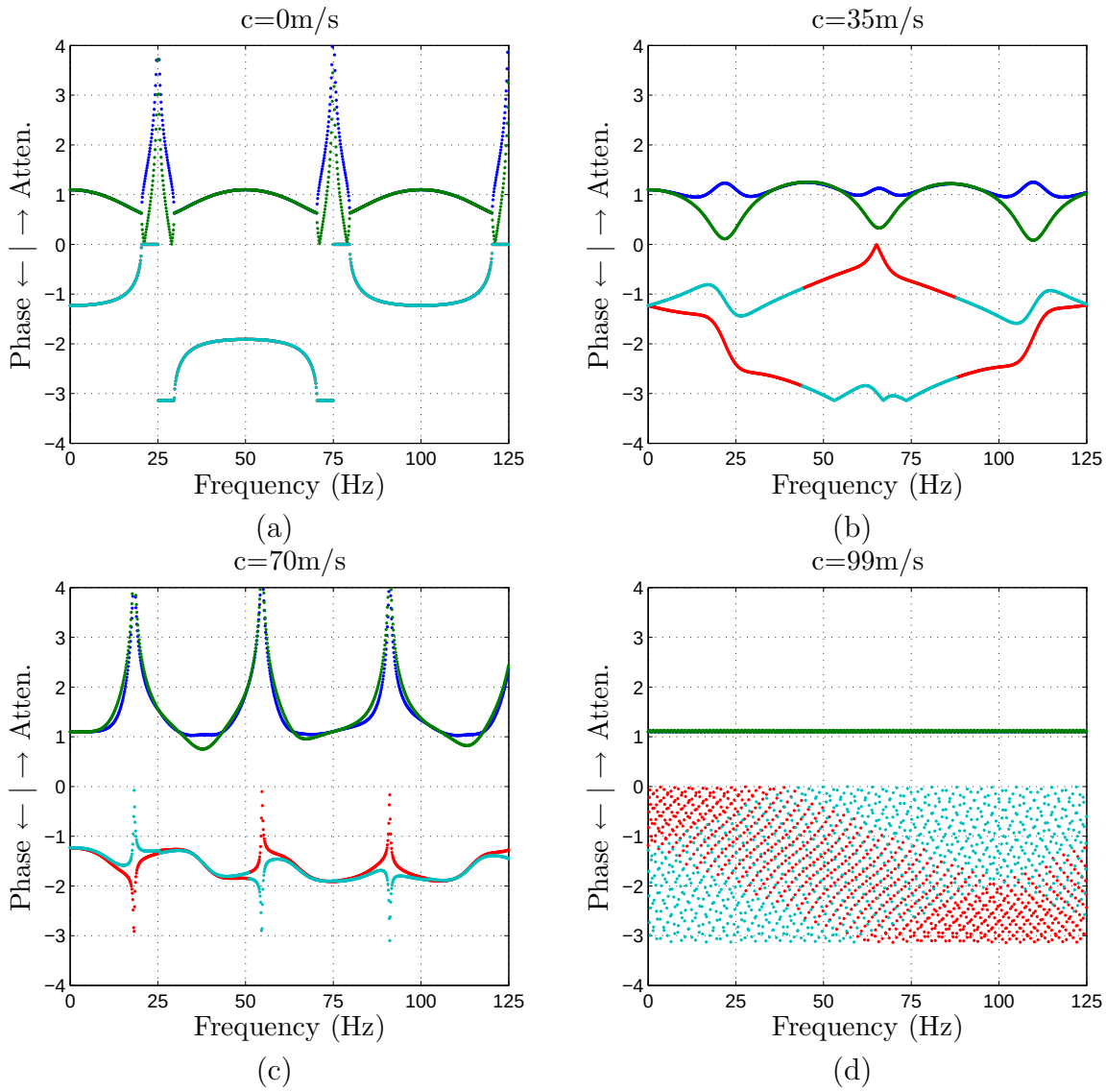

Figure 4.28: Dispersion curves for the periodic cell of the axially moving cable with periodic elastic supports with linear elastic constant $s = 10^5\, N/m$ varying the moving speed (a) the static system ($c = 0\, m/s$), (b) $c = 35\, m/s$, (c) $c = 70\, m/s$ and (d) $c = 99\, m/s$

Observing the dispersion curves shown on Fig. 4.26, Fig. 4.27,and Fig. 4.28 increasing speed for this case increases the imaginary part, which indicates that the rate of spatial decay for a wave propagating through the structure also increases with speed and with frequency.

4.6 Chapter remarks

In this chapter the analyzes and the results for the four studied models were presented. The axially moving cable with simple supports was analyzed by using the SEM and the FEM. The axially moving cable with elastic foundation had two configurations, the boundary elastic foundation and the middle elastic foundation, both using the SEM. The axially moving cable with periodic elastic foundation was modeled using the SEM and the spectral matrix was transformed into transfer matrix.

In all models observed the increasing speed decreases the resonance frequencies and the anti-resonance frequencies. In the elastic foundation and the periodic elastic foundation increasing the linear elastic constant, s, increases the resonance frequency however it has no influence on the anti-resonance frequency of the models.

5. Conclusions and recommendations for further work

5.1 Conclusions

The critical speed is not affected by any of the configurations (elastic foundation or periodic elastic foundation). All the configuration studied had the same critical speed $100\,m/s$.

The axially moving cable with simple supports was modeled using both spectral element and Finite Element Methods. In both models the results showed that the increasing speed decreases all the resonance and anti-resonance frequencies.

The axially moving cable with elastic foundation was modeled using two configurations, the boundary elastic foundation and the middle elastic foundation. For both configurations it was found that below $s = 10^3\,N/m$ the elastic foundation do not interfere significantly in the resonance and after $s = 10^6\,N/m$ it inhibits the transversal displacement. Between 10^3 and $10^6\,N/m$ increasing the linear elastic constant, s, increases the resonance frequency however it has no influence on the anti-resonance frequency of the model. The impact of the elastic foundation is greatest at low frequency, where the stiffness of the system has biggest influence. The influence of the speed is the same as in the simple supported model, increasing speed decreases the resonance and anti-resonance frequency. The boundary elastic foundation model present a damping effect with increasing speed, such damping is best expressed at high frequency and with lower values of the linear elastic constant, s, and it is caused by the different boundary conditions of this configuration.

The axially moving cable with periodic elastic foundation was modeled using the Spectral

Element Method and the results showed that the influence of the periodic elastic foundation on the model occur between 10^3 and $10^6\,N/m$, with the linear elastic constant increase all propagation regions become narrower and shift to the right. Before $10^3\,N/m$ it has no influence on the propagation region and after $10^6\,N/m$ the node behavior is similar to a fixed node.

The periodic cell of this configuration was analyzed using the transfer matrix, to evaluate the attenuation and propagation regions using the dispersion relation and it was possible to conclude that the imaginary part increases with speed and also with frequency, which indicates that the rate of spatial decay for a wave propagating through the structure also increases with speed and with frequency.

5.2 Recommendations for further work

A possible approach for further work could consider deepening the understanding of the dynamic behavior through the transfer matrix and to continue the study on the periodic systems. Also could consider to develop the transfer matrix from the explicit dynamic stiffness matrix for the transverse oscillation of an axially moving cable in the literature. Another direction for further work could consider to experimentally study the axially moving cable with simple supports and compare the numerical results with experimental tests. One more possible approach could consider to study the stability of the system through analysis of the state space matrix eigenvalues with the Finite Element Method.

Bibliography

W. Ames, S. Lee, and J. Zaiser. Non-linear vibration of a traveling threadline. *International Journal of Non-linear mechanics*, 3(4):449–456, 1968.

A. Ashari and N. Stephen. On wave propagation in repetitive structures: Two forms of transfer matrix. *Journal of Sound and Vibration*, 439:99–112, 2019.

N. Banichuk, S. Ivanova, J. Jeronen, and T. Tuovinen. Periodic spectral instability analysis of axially moving beam with elastic supports. *J. Struct. Mech*, 47(1):1–16, 2014.

N. Banichuk, A. Barsuk, S. Ivanova, J. Jeronen, E. Makeev, and T. Tuovinen. Vibrations of a continuous web on elastic supports. *Mechanics Based Design of Structures and Machines*, 46(1):1–17, 2018.

D. Beli. Vibration attenuation and elastic wave manipulation in periodic structures using band gaps and nonreciprocity: Atenuação de vibrações e manipulação de ondas elásticas em estruturas periódicas utilizando bandas proibidas e não reciprocidade. 2018.

R. Bhat, G. Xistris, and T. Sankar. Dynamic behavior of a moving belt supported on elastic foundation. *Journal of Mechanical Design*, 104(1):143–147, 1982.

L. Brillouin. Wave propagation in periodic structures: electric filters and crystal lattices. 1953.

J.-S. Chen. Natural frequencies and stability of an axially-traveling string in contact with a stationary load system. 1997.

J. Cho and U. Lee. An fft-based spectral analysis method for linear discrete dynamic systems with non-proportional damping. *Shock and Vibration*, 13(6):595–606, 2006.

R. W. Clough. The finite element method in plane stress analysis. In *Proceedings of 2nd ASCE Conference on Electronic Computation, Pittsburgh Pa., Sept. 8 and 9, 1960*, 1960.

J. Doyle. A spectrally formulated finite element for longitudinal wave propagation. *International Journal of Analytical and Experimental Modal Analysis*, 3:1–5, 1988.

J. F. Doyle. *Wave propagation in structures: spectral analysis using fast discrete fourier transforms, mechanical engineering series.* 1997.

C. A. Felippa. A historical outline of matrix structural analysis: a play in three acts. *Computers & Structures*, 79(14):1313–1324, 2001.

J. Fish and T. Belytschko. *A first course in Finite Element.* Grupo Gen-LTC, 2000.

A. Foehr, O. R. Bilal, S. D. Huber, and C. Daraio. Spiral-based phononic plates: From wave beaming to topological insulators. *Physical review letters*, 120(20):205501, 2018.

N. V. Gaiko and W. T. van Horssen. On the transverse, low frequency vibrations of a traveling string with boundary damping. *Journal of Vibration and Acoustics*, 137(4), 2015.

P. J. P. Gonçalves. *Dynamic analysis and active control of lattice structures.* PhD thesis, University of Southampton, 2007.

M. R. Gosz. *Finite element method: applications in solids, structures, and heat transfer.* CRC Press, 2017.

M. I. Hussein, M. J. Leamy, and M. Ruzzene. Dynamics of phononic materials and structures: Historical origins, recent progress, and future outlook. *Applied Mechanics Reviews*, 66(4), 2014.

A. Hvatov and S. Sorokin. Free vibrations of finite periodic structures in pass-and stop-bands of the counterpart infinite waveguides. *Journal of Sound and Vibration*, 347:200–217, 2015.

Indiamart. Power transmission belt, Access 07032020. URL `bit.ly/333DfBC`.

F. Jacob and B. Ted. *A first course in finite elements.* Wiley, 2007.

L. Junyi and D. Balint. An inverse method to determine the dispersion curves of periodic structures based on wave superposition. *Journal of Sound and Vibration*, 350:41–72, 2015.

J. Kim, J. Cho, U. Lee, and S. Park. Modal spectral element formulation for axially moving plates subjected to in-plane axial tension. *Computers & Structures*, 81(20):2011–2020, 2003.

K. Kwon and U. Lee. Spectral element modeling and analysis of an axially moving thermoelastic beam-plate. *Journal of Mechanics of Materials and Structures*, 1(4):605–632, 2006.

R. Langley. A transfer matrix analysis of the energetics of structural wave motion and harmonic vibration. *Proceedings of the Royal Society of London. Series A: Mathematical, Physical and Engineering Sciences*, 452(1950):1631–1648, 1996.

L. Le-Ngoc and H. McCallion. Dynamic stiffness of an axially moving string. *Journal of sound and vibration*, 220(4):749–756, 1999.

C. L. Lee and N. C. Perkins. Experimental investigation of isolated and simultaneous internal resonances in suspended cables. *Journal of vibration and acoustics*, 117(4):385–391, 1995.

U. Lee. Equivalent continuum representation of lattice beams: spectral element approach. *Engineering Structures*, 20(7):587–592, 1998.

U. Lee. Vibration analysis of one-dimensional structures using the spectral transfer matrix method. *Engineering structures*, 22(6):681–690, 2000.

U. Lee. Dynamic characterization of the joints in a beam structure by using spectral element method. *Shock and Vibration*, 8(6):357–366, 2001.

U. Lee. *Spectral element method in structural dynamics*. John Wiley & Sons, 2009.

U. Lee and I. Jang. On the boundary conditions for axially moving beams. *Journal of Sound and Vibration*, 306(3-5):675–690, 2007.

U. Lee and H. Oh. Dynamics of an axially moving viscoelastic beam subject to axial tension. *International Journal of Solids and Structures*, 42(8):2381–2398, 2005.

U. Lee, J. Kim, and H. Oh. Spectral analysis for the transverse vibration of an axially moving timoshenko beam. *Journal of Sound and Vibration*, 271(3-5):685–703, 2004.

Y. Li, D. Aron, and C. D. Rahn. Adaptive vibration isolation for axially moving strings: theory and experiment. *Automatica*, 38(3):379–390, 2002.

X.-Y. Mao, H. Ding, and L.-Q. Chen. Forced vibration of axially moving beam with internal resonance in the supercritical regime. *International Journal of Mechanical Sciences*, 131: 81–94, 2017.

D. Mead. Wave propagation in continuous periodic structures: research contributions from southampton, 1964–1995. *Journal of sound and vibration*, 190(3):495–524, 1996.

C. Mote Jr. Dynamic stability of an axially moving band. *Journal of the Franklin Institute*, 285(5):329–346, 1968.

S. Naguleswaran and C. Williams. Lateral vibration of band-saw blades, pulley belts and the like. *International Journal of Mechanical Sciences*, 10(4):239–250, 1968.

G. Narayanan and D. Beskos. Use of dynamic influence coefficients in forced vibration problems with the aid of fast fourier transform. *Computers & Structures*, 9(2):145–150, 1978.

G. F. Nehemy, P. J. P. Gonçalves, and E. A. C. Sousa. Dynamic behavior of axially moving systems with elastic supports. 01 2019. doi: 10.26678/ABCM.COBEM2019.COB2019-0309.

H. Oh, U. Lee, and D.-H. Park. Dynamics of an axially moving bernoulli-euler beam: Spectral element modeling and analysis. *KSME international journal*, 18(3):395–406, 2004.

H. Öz. Natural frequencies of axially travelling tensioned beams in contact with a stationary mass. *Journal of sound and vibration*, 259(2):445–456, 2003.

H. Öz and M. Pakdemirli. Vibrations of an axially moving beam with time-dependent velocity. *Journal of Sound and Vibration*, 227(2):239–257, 1999.

R. Parker. Supercritical speed stability of the trivial equilibrium of an axially-moving string on an elastic foundation. *Journal of Sound and Vibration*, 221(2):205–219, 1999.

F. Pellicano and F. Vestroni. Complex dynamics of high-speed axially moving systems. *Journal of Sound and Vibration*, 258(1):31–44, 2002.

F. Pellicano, A. Fregolent, A. Bertuzzi, and F. Vestroni. Primary and parametric non-linear resonances of a power transmission belt: experimental and theoretical analysis. *Journal of Sound and Vibration*, 244(4):669–684, 2001.

N. Perkins. Linear dynamics of a translating string on an elastic foundation. *Journal of Vibration and Acoustics*, 112(1):2–7, 1990.

T. H. Pian and P. Tong. Finite element methods in continuum mechanics. In *Advances in applied mechanics*, volume 12, pages 1–58. Elsevier, 1972.

S. Rizzi and J. Doyle. A spectral element approach to wave motion in layered solids. *Journal of Vibration and Acoustics*, 114(4):569–577, 1992.

Royal Packing. Paperboard sheeter, Access 07032020. URL `bit.ly/3328DjD`.

S. Rubin. Mechanical immittance-and transmission-matrix concepts. *The Journal of the Acoustical Society of America*, 41(5):1171–1179, 1967.

R. Sack. Transverse oscillations in travelling strings. *British Journal of Applied Physics*, 5(6): 224, 1954.

M. Shen and W. Cao. Acoustic bandgap formation in a periodic structure with multilayer unit cells. *Journal of Physics D: Applied Physics*, 33(10):1150, 2000.

V. S. Sorokin and J. J. Thomsen. Wave propagation in axially moving periodic strings. *Journal of Sound and Vibration*, 393:133–144, 2017.

C. Spyrakos and D. Beskos. Dynamic response of frameworks by fast fourier transform. *Computers & Structures*, 15(5):495–505, 1982.

C. Tan and S. Ying. Dynamic analysis of the axially moving string based on wave propagation. 1997.

Timberwolf Tools. Band saw, Access 07032020. URL `bit.ly/2W2DkUi`.

M. J. Turner, R. W. Clough, H. C. Martin, and L. Topp. Stiffness and deflection analysis of complex structures. *journal of the Aeronautical Sciences*, 23(9):805–823, 1956.

J. Wickert and C. Mote. Current research on the vibration and stability of axially-moving materials. *Vibration Inst., The Shock and Vibration Digest*, 20(5):3–13, 1988.

C. Xia, Y. Wu, and Q. Lu. Experimental study of the nonlinear characteristics of an axially moving string. *Journal of Vibration and Control*, 21(16):3239–3253, 2015.

B. Yang and C. Mote Jr. Vibration control of band saws: Theory and experiment. *Wood science and technology*, 24(4):355–373, 1990.

Y. Yong and Y. Lin. Propagation of decaying waves in periodic and piecewise periodic structures of finite length. *Journal of Sound and Vibration*, 129(1):99–118, 1989.

H. Zhang and L. Chen. Vibration of an axially moving string supported by a viscoelastic foundation. *Acta Mechanica Solida Sinica*, 29(3):221–231, 2016.

J. Zhou, K. Wang, D. Xu, and H. Ouyang. Local resonator with high-static-low-dynamic stiffness for lowering band gaps of flexural wave in beams. *Journal of Applied Physics*, 121 (4):044902, 2017.

W. Zhu, C. Mote Jr, and B. Guo. Asymptotic distribution of eigenvalues of a constrained translating string. 1997.

A. Adition of mass, spring and damper on the impedance matrix

The inclusion of a mass, spring or damper component on a node of an impedance matrix is done throughout adding the component's impedance at the matrix node. The component's impedance is obtained as

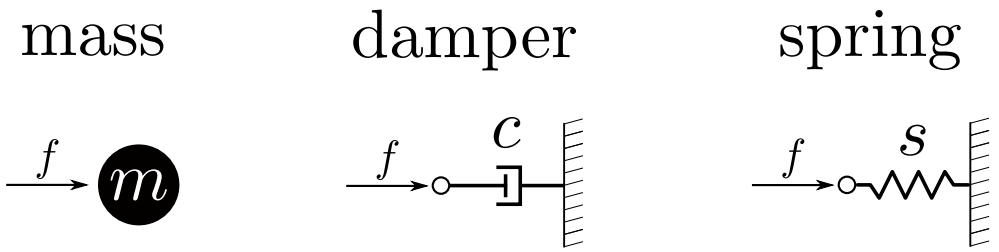

Figure A.1: Components of mass, damper and spring.

Considering isolated mass, damper and spring and an harmonic force acting on each one, as showed on Fig A.1. The harmonic response for x and its derivatives are given by

$$x = Xe^{j\omega t}\ ,\ \dot{x} = j\omega Xe^{j\omega t}\ ,\ \ddot{x} = -\omega^2 Xe^{j\omega t}$$

For the mass,

$$\begin{aligned} f =& m\ddot{x} \\ Fe^{j\omega t} =& -\omega^2 mXe^{j\omega t} \\ \frac{X}{F} =& -\omega^2 m \end{aligned}$$

For the damper,

$$\begin{aligned} f &= c\dot{x} \\ Fe^{j\omega t} &= j\omega cXe^{j\omega t} \\ \frac{X}{F} &= j\omega c \end{aligned}$$

For the spring,

$$\begin{aligned} f &= sx \\ Fe^{j\omega t} &= sXe^{j\omega t} \\ \frac{X}{F} &= s \end{aligned}$$

Thus, to insert a mass in an impedance matrix node it must be added $-\omega^2 m$, for the damper it must be added $j\omega c$ and for the spring it must be added s.